STRUCTURAL ANALYSIS OF DEGENERATIVE CARTILAGE USING AN INFRARED FIBER OPTIC PROBE

by

PAUL A. WEST

A disseration submitted to the Graduate Faculty in Engineering in partial fulfillment of the requirements for the degree of Doctor of Philosophy, The City University of New York

2002

This manuscript has been read and accepted for the Graduate Faculty in Engineering in satisfaction of the dissertation requirement for the degree of Doctor of Philosophy.

05/01/02
Date

S C Cowin
Chair of Examining Committee

05/01/02
Date

Murtaza K. Kaysir
Executive Officer

NANCY CAMACHO Ph.D

PETER TORZILLI Ph.D

SUSANNAH FRITTON Ph.D

ALI SADEGH Ph.D

Supervisory Committee

The City University of New York

THE CITY UNIVERSITY OF NEW YORK

Abstract

STRUCTURAL ANALYSIS OF DEGENERATIVE CARTILAGE USING AN INFRARED FIBER OPTIC PROBE

by

PAUL A. WEST

Advisers: Professor Steve C. Cowin (Mentor)
Dr. Nancy P. Camacho (Co-mentor)

Osteoarthritis (OA) is a progressively disabling musculoskeletal disease characterized by degeneration of the articular cartilage. The current understanding within the field of orthopedics is that the progression of OA is accompanied by structural and compositional changes within the tissue due to collagen damage at the articular surface and loss of proteoglycans (PG) through the articular surface. This leads to a loss of the articular cartilage, followed by sclerosis of the subchondral bone and the formation of subchondral bone cysts and osteophytes.

Currently, a significant complication in the treatment of osteoarthritis is the inability to diagnose the disease process at an early stage. While macroscopic, end-stage cartilage damage can be recognized by radiographic methods, early stages of OA that involve disruption of the cartilage but without any obvious surface damage are much more difficult to identify.

FT-IR spectroscopy is currently emerging as a technique that is being increasingly utilized for the analysis of proteins in biological tissues. In this thesis, a new alternative for IR sampling utilizes an infrared fiber optic probe (IFOP) in the investigation of spectral changes related to early articular cartilage degradation. Here we show that

molecular changes associated with the degradation of the superficial zone type II collagen network can be monitored by FTIR spectroscopy. Specifically in the 1800-1000 cm^{-1} wavenumber region, we have demonstrated that there are spectral changes associated with the degradation of type II collagen. These changes are consistent between normal and arthritic cartilage, both in human and animal studies. This evidence is also further corroborated when collagenase treated articular cartilage is compared to normal cartilage.

We envision the use of the IFOP as a diagnostic tool that can be used in conjunction with arthroscopy for the evaluation of cartilage integrity and also for assessing the integration of tissue engineered cartilage.

ACKNOWLEDGEMENTS

I am extremely grateful to the many people who have provided me with positive support during my quest for a doctoral degree. Without their help and encouragement over the years, I would not have been able to get to this point

First, I would like to thank Nancy Camacho whose brilliance, foresight, and continuous guidance has served as a means of inspiration. I would like to thank Mathias Bostrom, Xu Yang and Jian Hao Lin for their never-ending desire to help.

Thanks to Matthew Griffith and Divya Diwan.

A very special thanks to Peter Torzilli and the Laboratory for Soft Tissue Research. Their help has proven invaluable.

I owe a great deal to Adele Boskey, Steve Doty, Lefty Paschalis and the entire fourth floor Research Division for their patient help over the years.

Thanks to my Ph.D. committee members, Steve Cowin, Susannah Fritton, Ali Sadegh and Richard Mendelsohn for their encouragement and guidance.

I am grateful to many people in the Mechanical Engineering Department at City College who have shown me love and support over the years. Among them, Charles Watkins, Steve Cowin, Sheldon Weinbaum, Feridun Delale, Latif Jiji, and Gerard Lowen.

To my mother who has encouraged me and supported me. To my wife Dianna, who has shown untiring patience and resolve, and to my children, thanks for showing me the meaning of life.

Last but not least, a very special thanks to Sherwood Menkes who is no longer with us, but whose encouragement has made me aspire for greater things.

TABLE OF CONTENTS

List of Tables

List of Illustrations

CHAPTER I

INTRODUCTION

Articular cartilage is a poroviscoelastic connective tissue that lines the articulating ends of diarthrodial joints (Fig.1-1). It provides excellent lubrication, energy absorption, and wear characteristics, while sustaining loads of up to 10 times body weight for up to eight decades (1). These impressive biomechanical features exist in an aneural and avascular living tissue in which mechanical integrity is continuously maintained by biological synthesis and repair.

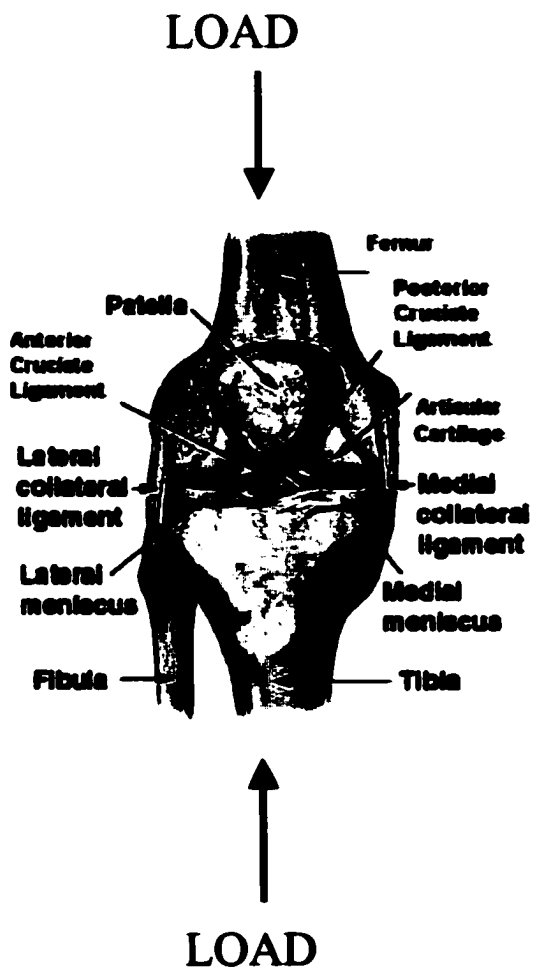

Figure 1-1: Knee anatomy (adapted from www.hurt911.org).

1. Figure 1-2: Cartilage zones (adapted from Orthopaedic Basic Science. Edited by Sheldon R. Simon, MD. American Academy of Orthopaedic Surgeons, 1994).

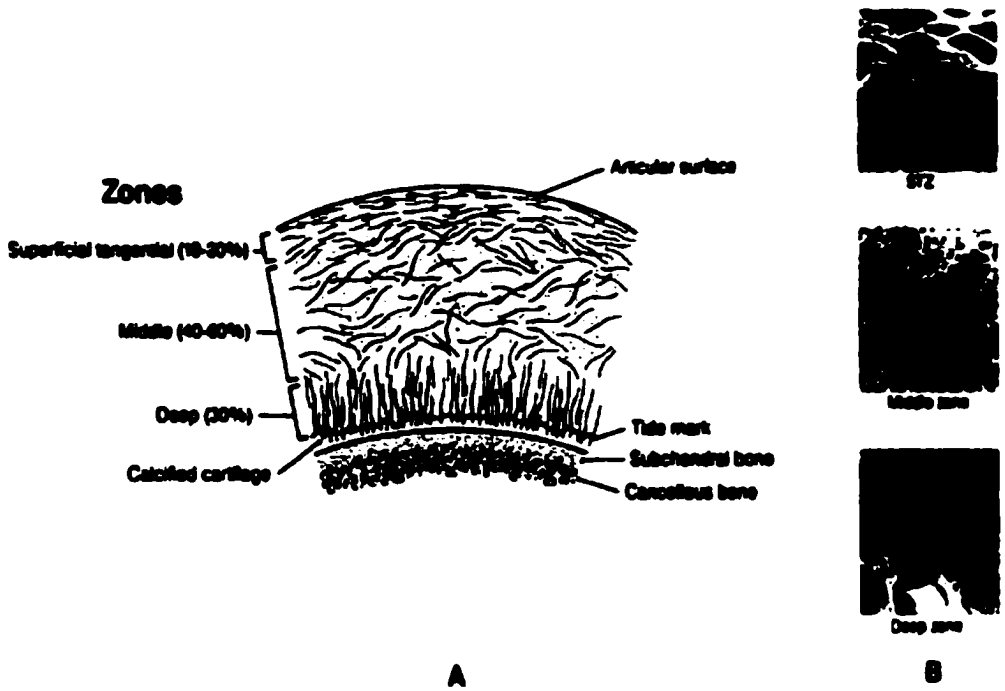

There are four spatial zones in articular cartilage:

the superficial, transitional, deep, and calcified zones (Fig. 1-2). Chondrocytes, the cells present in cartilage, are responsible for the production, organization, and maintenance of the extracellular matrix (ECM) within each zone. This extracellular matrix has a composite-like architecture that is primarily composed of water (70-80%) and macromolecules: type II collagen (15-25%) and proteoglycans (5-25%) (2). These three major components act together to determine the mechanical properties of cartilage. The main function of type II collagen is to provide reinforcement within the articular cartilage ECM. Each molecule consists of three polypeptide chains (α1 chains) wound into a helical arrangement ~ 300-nm long. Within the ECM, these molecules self-assemble in a staggered array via an entropy-driven process to form collagen fibrils. Collagens type IX and XI contribute to the organization and mechanical stability of the type II collagen

fibrils. Within these fibrils, hydroxylysyl pyridinoline residue intermolecular cross-links are formed to provide the structural stability necessary for cartilage function (3). The diameter of type II collagen fibrils range from 50 to over a 100 nm in mature articular cartilage. The collagen fibrils function to trap and constrain the large aggregating hydrophilic proteoglycan (PG) molecules called aggrecan (Fig. 1-3). Aggrecan makes up ~ 90% of all the proteoglycans in articular cartilage. It consists of a large 2.25 kd three domain (G1,G2,G3) protein core to which polyanionic chondrotin sulfate and keratan sulfate glycosaminoglycan chains are attached. With the aid of a link protein, up to 800 aggrecan molecules may bind to hyaluronate to form a large water-attracting aggregate. This water attraction causes osmotic swelling in aggrecan which is balanced by the collagen fibers (3). Under normal physiologic conditions, when a compressive force is applied, fluid is squeezed out of the cartilage. When the fluid is being squeezed out, drag forces are created between the fluid and the solid matrix that increase with increasing compression and make it more difficult to exude water. This phenomenon increases the stiffness of cartilage as the rate of loading is increased.

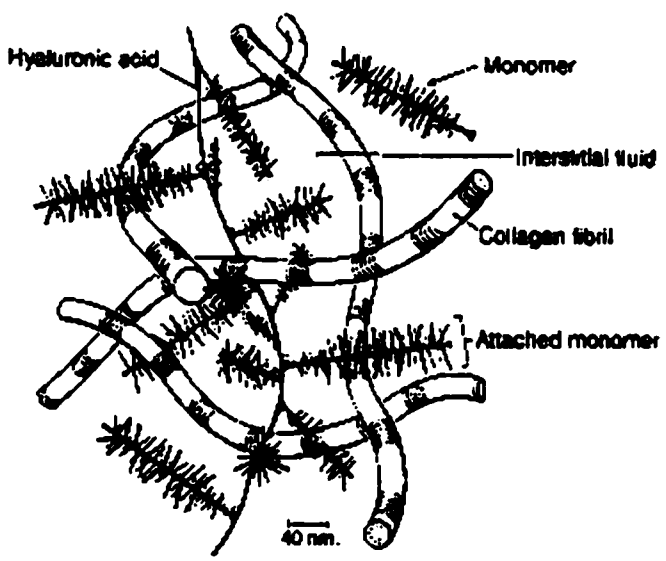

A

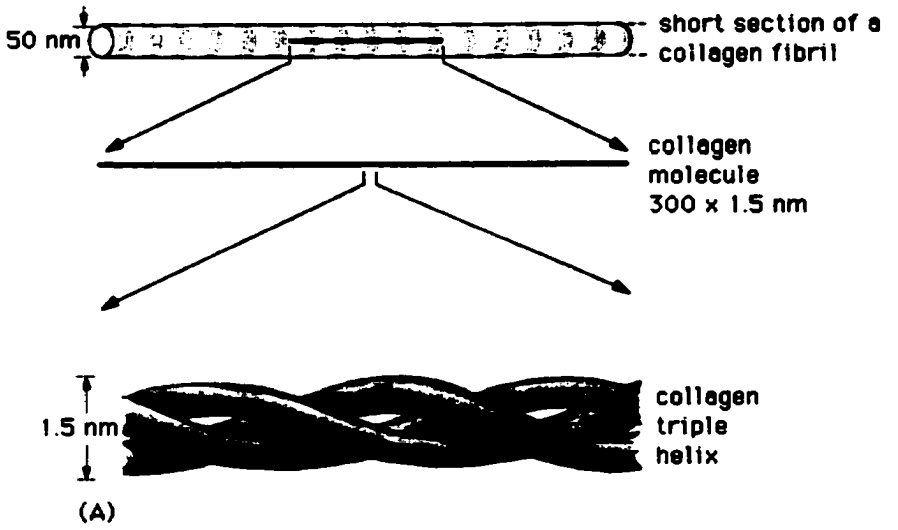

B

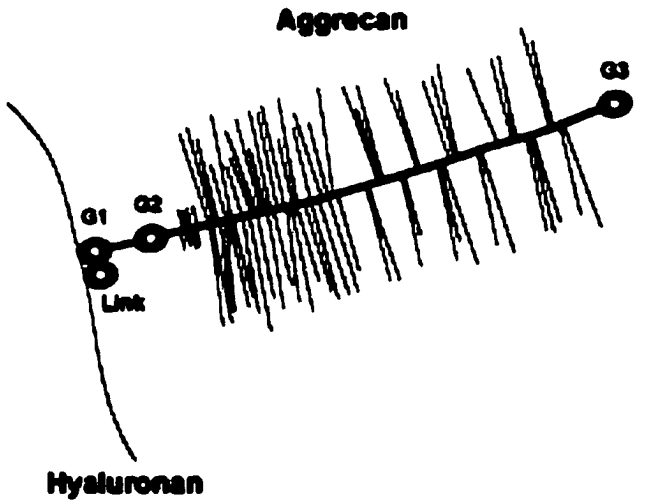

C

Fig. 1-3: A-Articular cartilage ECM (adapted from Orthopaedic Basic Science. Edited by Sheldon R. Simon, MD. American Academy of Orthopaedic Surgeons, 1994). B-Collagen molecule (adapted from medinfo.com). C-Aggrecan

In cartilage the superficial zone is the thinnest zone (10-20%). It is composed of flattened chondrocytes, a low proteoglycan content, high water content, and densely packed collagen fibers aligned parallel to the articular surface. The transitional zone (40-60%) is composed of rounded chondrocytes, randomly arranged collagen fibers, and increased proteoglycan content. In the deep zone (~ 30%) the collagen fibers are generally oriented normal to the articular surface, the proteoglycan content remains high, while the cell volume is at its lowest. Surrounding each chondrocyte, the extracellular matrix is subdivided into the pericellular, territorial, and interterritorial regions. Mechanical influences in the extracellular matrix can be sensed by the chondrocytes, which respond by effecting a balance between anabolism and catabolism. This continual remodeling replaces matrix macromolecules that are lost through degradation. Maintaining the biomechanical properties of articular cartilage depend on the interaction between the chondrocytes and the extracellular matrix.

The primary function of articular cartilage is to facilitate the efficient transmission of mechanical loads across the articulating joint. The ability of cartilage to function correctly depends on the biomechanical properties of the tissue. Any alteration in the structural configuration of cartilage will affect its ability to perform effectively. Preserving the integrity of the tissue is thus critical for normal function, and it is the failure of the biomechanical and biological properties of articular cartilage that is widely believed to be the fundamental cause of osteoarthritis and other joint diseases.

Osteoarthritis (OA) is a progressively disabling musculoskeletal disease characterized by degeneration of articular cartilage. It consists of a progressive loss of the articular cartilage, followed by sclerosis of the subchondral bone and the formation of subchondral bone cysts and osteophytes. It currently affects approximately 14% of the

United States population ages 25 to 74, and is considered the leading cause of long-term disability among adults (4). The joint degeneration that causes osteoarthritis occurs most frequently in the hand, foot, knee, and hip joints. Progressive degeneration of the joint structure not only reduces patient mobility, but also has significant economic repercussions. The combined costs of medical care (diagnostic studies, doctor visits, medications, surgery, and physical therapy) and non-medical costs create a huge burden on individuals, medical care systems, and the national economy (5). Other than joint surgery, there is currently no treatment that provides symptomatic relief or improved mobility in patients with osteoarthritis (6,7). The limited effectiveness of current arthritic therapies has thus stimulated scientists to continue to seek new treatments. Evaluating the success of these new treatments require an understanding of the role of genetics, diagnosis, etiology, development, and progression of osteoarthritis.

In osteoarthritis, the progression of disease can be divided into three overlapping stages: extracellular matrix changes, chondrocyte sensing and response to tissue changes, and, finally, the decline of the chondrocyte response (5,7-10). The first stage may occur as a result of mechanical trauma, joint inflammation, or as a result of changes in the ability of the chondrocytes to maintain the extracellular matrix. The second stage begins when the chrondrocytes sense matrix changes, and stimulate a cellular response characterized by cell proliferation, anabolism and catabolism. Failure of the chondrocytes to stabilize or restore lost matrix components leads to the third stage in the development of osteoarthritis, where a decline in the number of chondrocytes and the chondrocyte response leads to the progressive loss of articular cartilage (7,10). Typically the onset of osteoarthritis is characterized by the upregulation of specific metalloproteinases (MMPs), primarily collagenase and stromelysin that target type II collagen and aggrecan,

respectively. These enzymes are synthesized by the chondrocytes and function to degrade the matrix proteins. Collagenase cleaves the triple helix into ¼ and ¾ length fragments, while stromelysin cleaves the protein core between the G1 and G2 domains (11). Progressive collagen disorganization and proteoglycan loss accompany disease progression.

Currently, a significant complication in the treatment of osteoarthritis is the inability to diagnose the disease process at an early stage. While macroscopic, later-stage cartilage damage such as lacerations, ruptures and chondral fractures can be recognized via existing technology (12), early stages of OA that involve disruption of the cartilage but with no obvious mechanical damage are much more difficult to identify. In this thesis, cartilage surface changes will be graded visually using the Collins scale (13). Grade 1 indicates very early fibrillation in the absence of macroscopic changes on the articular surface while grade 3 represents extensive fibrillation, fissuring and cartilage thinning. Recent reports have detailed potential changes at the molecular level that may include changes in collagen (14,15) or proteoglycan (16,17) content and structure. Knowledge of these types of ultrastructural changes at an early stage would be extremely important during arthroscopic procedures where crucial decisions are made regarding salvaging or removing cartilage.

Fourier-transform infrared (FT-IR) spectroscopy is a technique based on molecular vibrations. An infrared spectrum is obtained by passing radiation through a sample and determining what fraction of the incident radiation is absorbed at a particular frequency. The frequency at which any peak in an absorption spectrum appears corresponds to the frequency of a vibration of a part of the sample molecule. IR spectroscopy is currently emerging as a technique that is being increasingly utilized for

the analysis of proteins in biological tissues (18-21). Also, recent advances in IR techniques, instrumentation, computational methods, data acquisition times and protein band assignments have significantly improved the potential of IR spectroscopy as an analytical tool (22). Information on the quantity, structure, and interactions of these molecules with other tissue components may be obtained from such studies. However, most of these studies were limited by the requirement of having to perform the analyses ex vivo (23).

A new alternative for IR sampling utilizes an infrared fiber optic probe (IFOP). The recent availability of infrared transmitting fibers enables more flexible sampling approaches than have previously been utilized. We envision the use of the IFOP as an arthroscopic diagnostic tool for joint diseases and other injuries which lead to joint degeneration. This will permit *in situ* quantitation of the primary molecular determinants of cartilage matrix degradation at the ultrastructural level. As a result, this new technology will facilitate the diagnosis, treatment and management of osteoarthritis and other joint diseases.

Infrared Fiber Optic Probe (IFOP):

The Infrared Fiber Optic Probe consists of a flexible fiber optic bundle composed of a mid-infrared transmitting "chalcogenide" glass (RemSpec Corp, Sturbridge, MA) equipped with an Mercury Cadmium Telluride (MCT) detector module coupled to a BRUKER spectrometer (BRUKER, Germany) (Fig. 1-4). The fiber optic bundle is approximately 1 meter in length and transmissive over the infrared region of 4000 - 900 cm^{-1}. IR sampling is achieved by the use of an ATR (attenuated total reflectance) crystal attached to the end of the fiber optic bundle.

Theory of Operation:

The IFOP system works by collecting and focusing collimated IR radiation exiting the FTIR spectrometer (BRUKER) external port into a bundle of optical fibers. The fiber optic bundle is then direct-coupled using patented technology to an ATR crystal. Within the crystal, the internally reflected beam is direct-coupled back into the fiber optic bundle and sent to the detector module. The detector module uses a photoconductive mercury cadmium telluride (MCT) detector/optical system. A lens mounted inside the dewar focuses the signal exiting the fiber optic bundle onto the detector element. The detector element then outputs an electrical signal, which is amplified and transmitted to the FTIR spectrometer for spectral processing. There are 19 fibers within the fiber optic bundle: 7 input IR radiation to the ATR crystal, while 12 pass radiation to the detector.

Attenuated Total Reflectance Spectroscopy (ATR):

Attenuated total reflectance spectroscopy utilizes the phenomenon of total internal reflection. Incident IR radiation at the interface between sample and crystal will undergo total internal reflection if the angle of incidence is greater than the critical angle. The critical angle is a function of the refractive indices of the two surfaces. Maxwell's theory states that when light propagates through a transparent, nonabsorbent medium, a standing evanescent wave is formed perpendicular to the totally reflective surface. If the underlying sample absorbs some of the radiation, the propagating wave interacts with the sample and becomes attenuated giving rise to attenuated total reflectance. The resultant attenuated radiation is measured and plotted as a function of the wavelength and gives rise to the absorption spectral characteristics of the sample. In order to increase the sensitivity, multiple reflections (bounces) are used.

For the standing evanescent wave, the amplitude of the electric field (E) decays exponentially with distance from the interface according to the equation:

$$E = E_0 \exp [-z/d_p] \qquad \text{Eq(1)}$$

where z is the distance from the interface into the sample, and d_p is the penetration depth.

The magnitude of the penetration depth (d_p) depends on the wavelength of the radiation, λ, the refractive index of the crystal, n_c, the refractive index of the sample, n_s, and the angle of incidence of the beam at the surface of the crystal, ϕ.

$$Dp = \lambda / 2\pi n_c[\sin^2\phi-(n_s/n_c)^2]^{1/2} \qquad \text{Eq(2)}$$

For most materials, $d_p < 10\ \mu m$.

FTIR and Articular Cartilage:

The primary infrared (IR) active proteins of articular cartilage are aggrecan (proteoglycan) and type II collagen. The primary absorbances attributed to collagen and aggrecan are shown in Table 1 and Fig. 1-5&6.

Table I: Infrared Frequencies of Collagen and Proteoglycan in Cartilage.

Bond Vibrations	Collagen	Proteoglycan(PG)
Amide I C=O stretch	1655 cm-1	1642 cm-1
Amide II C-N stretch, N-H bend combination	1550 cm-1	1560 cm-1
Amide III C-N stretch, N-H bend, C-C stretch/ Sulfate stretch (PG)	1240 cm-1	1240 cm-1
C-O-C, C-OH, C-C ring vibrations		1125, 1070, 1040, 1000, 950 cm-1

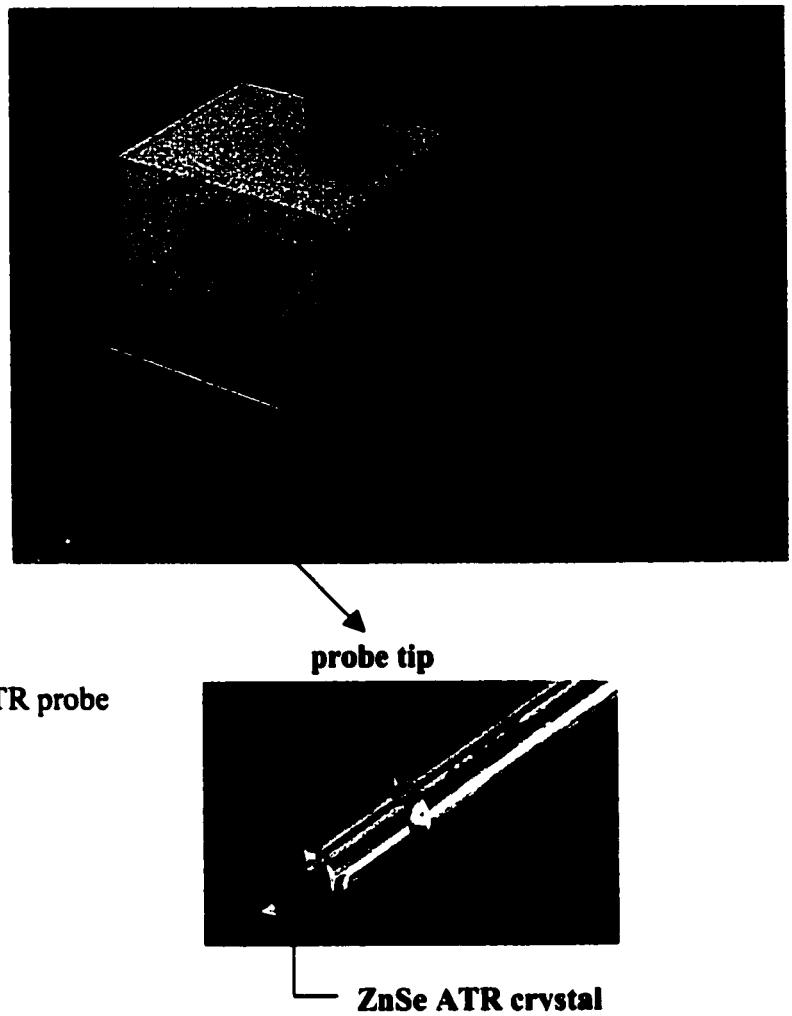

Fig. 1-4: ATR probe

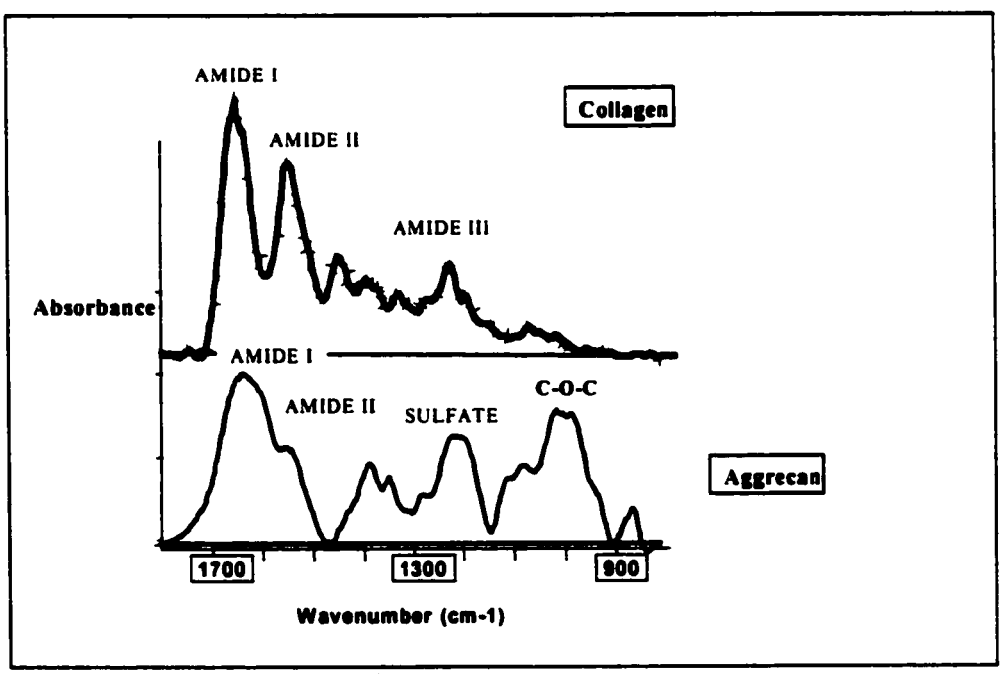

Fig 1-5: IR spectra of collagen and aggrecan.

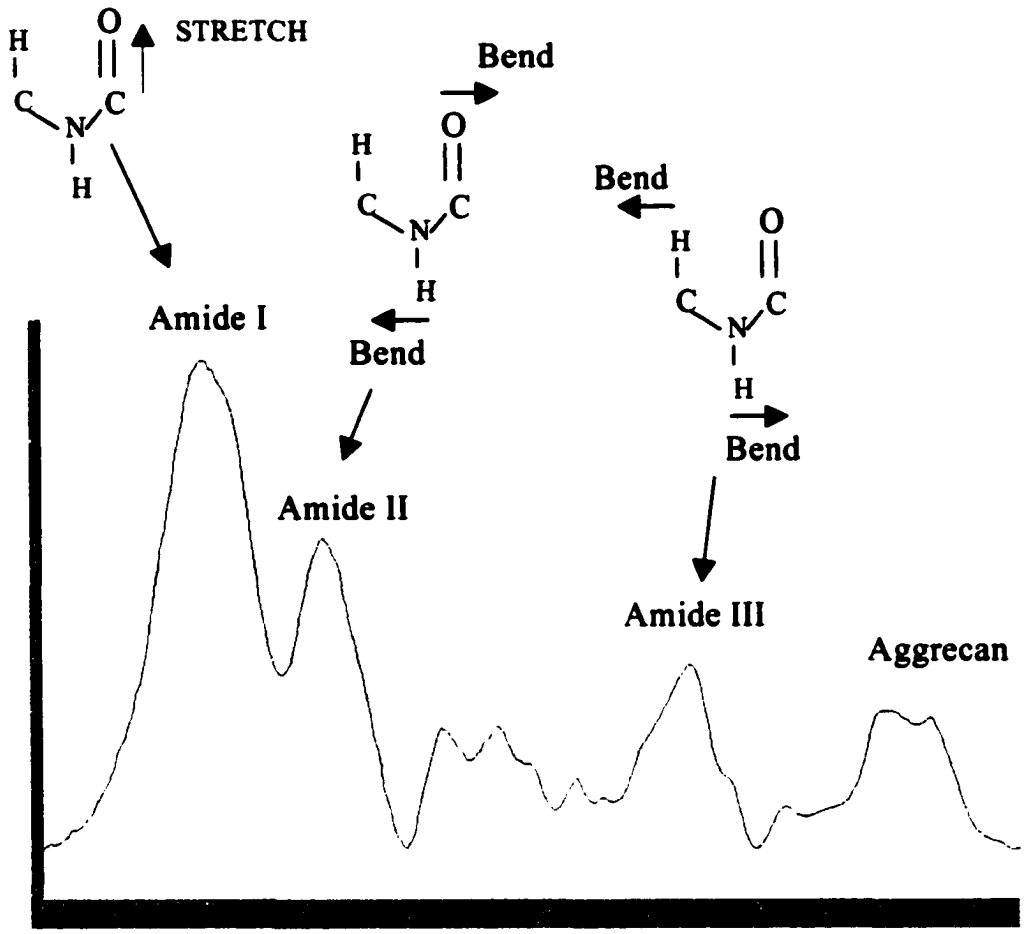

Fig. 1-6: Primary IR vibrations in articular cartilage.

Statistical Analysis (reference-statsoftinc.com)

Statistical data analysis is an important feature in any scientific experiment. In order to perform statistical data analysis however, one must first define the term statistics. Statistics defines the method used to collect, analyze, present, and interpret data. Statistics helps to quantify experimental differences and also helps to improve the prediction process. Statistical methods allow conclusions to be drawn from data that display experimental error. Statistics generally yield a probability value associated with a particular outcome.

Choosing the right statistical approach however depends on a number of factors: Mainly,

- The data source (how many variables?)
- Sample characteristics (are the samples (groups) independent?)
- Inferences that need to be made (what is the hypothesis or research question?)

Applying statistical methods to biological systems has been an ongoing challenge within the scientific community. This inherent difficulty lies in the high degree of variability found among living organisms. To combat this problem, large data sets are usually required. In this thesis, statistical analysis was done using means, standard deviations regression analysis and the paired T-test. Despite not having large data sets, satisfactory probability values were obtained. In the future, larger data sets and multivariate analysis will be used in order to make more precise predictions.

Mean: The mean is a measure of the "central tendency" of a variable. It is defined as the sum of the numbers divided by *n:*

For n values $x_1, x_2, ..., x_n$ the mean (M) = Σ x / n

Standard Deviation: The standard deviation is a measure of variability. The standard deviation of a set of n measurements $x_1, x_2, ..., x_n$, with the mean (M) is defined as the square root of the mean of the squares of the deviations; it is usually designated by the Greek letter sigma (σ).

$$\sigma = \sqrt{\{(1/n)\,\Sigma\,(xi - M)^2\}}$$

Regression Analysis: Regression analysis helps to determine if there is a useful relationship between two variables. It also determines the type of equation needed to describe the relationship. The R-square value is an indicator of how well the model fits

the data. In regression analysis, R can assume values between 0 and 1. An R-square value close to 1.0 indicates that we have accounted for almost all of the variability with the variables specified in the data set.

T-Test: The t-test is the most commonly used method to evaluate the differences in means between two groups. The groups can be independent or dependent. Theoretically, the t-test can be used even if the sample sizes are very small. A paired t-test is used to analyze groups that are linked. A paired t-test is a statistical test which is performed to determine if there is a reliable (statistically significant) difference between the means from two dependent groups. The *p*-value reported with a t-test represents the probability of error involved in accepting the research hypothesis about the existence of a difference. In many areas of research, information based on a p-value of < 0.05 is customarily treated as significant.

Purpose of this Thesis

The methodology of mid-infrared spectroscopy has long been applied to the study of biological systems. A major advantage of this method is that tissue in any physical state can be analyzed under any physiological condition. Also, with recent advances in FTIR technology, data acquisition times and computational methods, most biological tissues can be analyzed for ultrastructural and molecular changes associated with the onset of disease (22). In this thesis, we apply this technique to the development of an Infrared Fiber Optic Probe (IFOP) and to the pursuit of the detection of molecular changes associated with articular cartilage degradation.

Currently there are no commercially available techniques for the diagnosis and treatment of early degenerative joint disease: a very painful and disabling disease

characterized first by molecular/compositional changes in the collagen/proteoglycan extracellular matrix, followed by cartilage erosion and eventually subchondral bone damage (4). Here we show that molecular changes associated with the degradation of the superficial zone type II collagen network can be monitored by FTIR spectroscopy. Specifically in the 1800-1000 cm^{-1} wavenumber region, we have demonstrated that there are spectral changes associated with the degradation of type II collagen. These changes are consistent between normal and arthritic cartilage, both in human and animal studies. This evidence is also further corroborated when collagenase treated articular cartilage is compared to normal cartilage.

Our main goal is to use this new information in combination with a newly developed commercially available IR Fiber Optic Probe for the diagnosis of joint disorders. Such a system may be used in conjuction with arthroscopy for evaluation of cartilage integrity and also for assessing the integration of tissue engineered cartilage. Clearly, the ability of FTIR spectroscopy to potentially identify degenerative cartilage changes, coupled with its portability and cost effectiveness presents us with an advantage over other currently available diagnostic techniques.

This thesis is hereby organized as follows:

Chapter I: Introduction

Chapter II: Experimental Setup and Validation of the Infrared Fiber Optic Probe (IFOP)

Chapter III: FTIR Study of Model Compounds and Gels

Chapter IV: FTIR Evaluation of Genetically Modified Bovine Chondrocytes

Chapter V: Development of the Infrared Fiber Optic Sampling Methodology

Chapter VI: Observing the Effects of Stress Relaxation on the IFOP Spectral Quality

CHAPTER II

Experimental Setup and Validation of the Infrared Fiber Optic Probe (IFOP)

Experimental Setup

IFOP: The experimental setup consists of the infrared fiber optic probe connected to a BRUKER spectrometer (Bruker, Ettlingen, Germany) and a Remspec Mercury Cadmium Telluride (MCT) liquid nitrogen cooled detector (RemSpec Corp, Sturbridge, MA) (Fig. 2-1). In addition, we have a micrometer (resolution: 10μm) driven OptoSigma 65mm Z stage (travel:10mm), on which a platform (part A), Omega load cell, and a 7 mm diameter sample bath (part B) is attached. The load cell is connected to an Omega high performance strain gage indicator (meter) with Omega RS-232 Serial Communication connected to a Micron Pentium III computer. The load and IR data was acquired respectively using TalTech WinWedge v 1.2 (RS-232 16 bit) and BRUKER Opus NT v 3 software. Parts B & C had to be machined (Fig. 2-2). All data acquired by ATR from the IFOP (@ 4 cm^{-1} resolution) was averaged (212 scans), referenced to a saline background and Savitsky Golay 17 point smoothed.

Fig. 2-1A: Schematic of IFOP set-up.

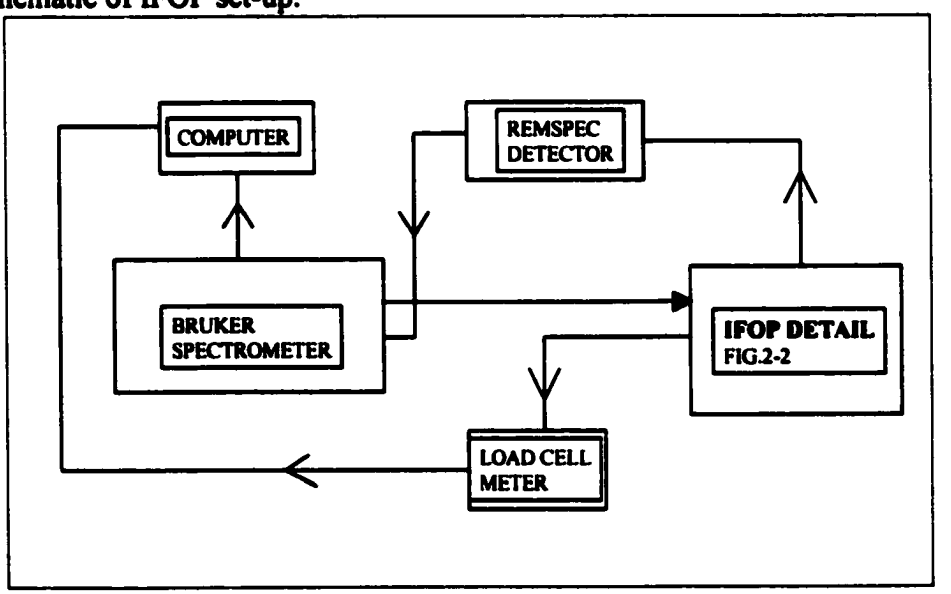

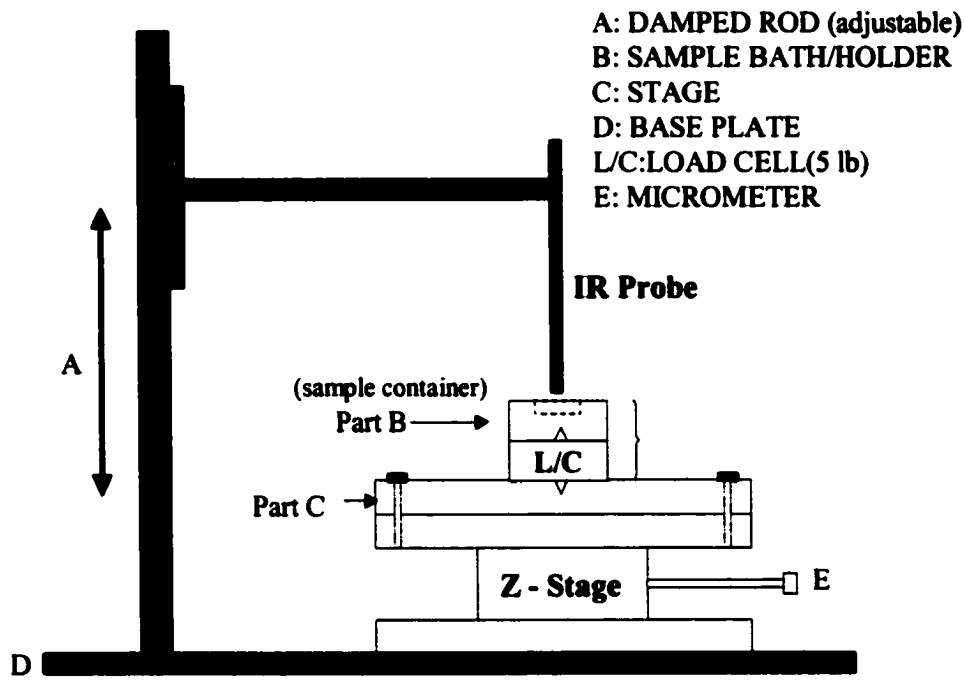

Fig.2-1B: Detail of IFOP set-up.

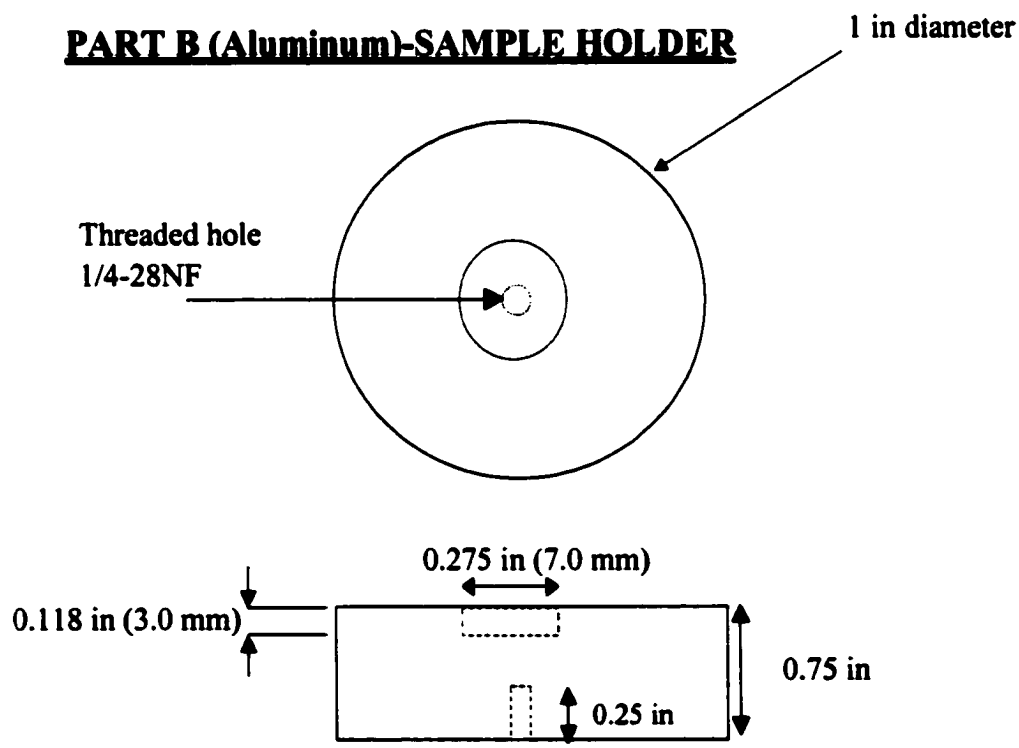

Fig.2-2A: Part B (sample holder)

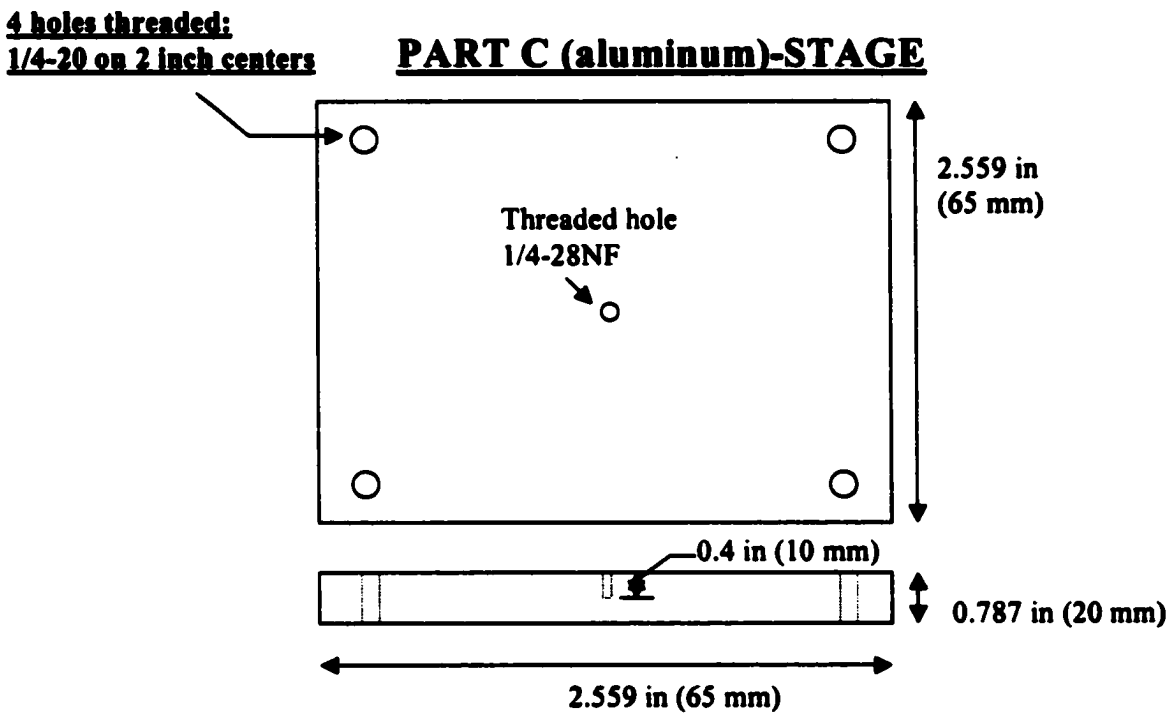

Fig.2-2B: Part C

FTIR IMAGING (FTIRI): FT-IR Imaging provides the gold standard to which IFOP determination was verified. The FT-IR Imaging system consists of a BioRad (Cambridge, MA) UMA 300A FTIR microscope with an FTS-60A step-scanning FTIR spectrometer and a liquid nitrogen cooled 64x64 MCT focal plane array (FPA) detector (Stingray Imaging Spectrometer). All data acquired by transmission (@ 8 cm^{-1} resolution under N_2 purge) from a 400 x 400 μm^2 sample region, resulting in 4,096 individual spectra.

IR data acquired using both methods outlined above were processed using Grams/32 AI v.6 (Galatic) and Win-IR Pro v.2.5 (Biorad).

Validation of the Infrared Fiber Optic Probe (IFOP)

A FT-IR investigation of the absorbances for the primary IR active cartilage proteins, aggrecan and type II collagen, is shown in figure 2-3. Comparison between the spectrum obtained using the IFOP (Fig. 2-4) at the articular surface and figure 2-3 reveals a distinct similarity with the IR spectrum of type II collagen. This clearly suggests that spectra acquired while using the IFOP at the articular surface is due to collagen within the superficial zone. Hence all spectral analysis will be referenced to collagen. Further comparison also revealed a shift from 1660 cm^{-1} to 1630 cm^{-1} in the amide I IFOP absorbance band (Fig 2-5) due to water interference with the ATR crystal. In light of this finding, no ultrastructural determination will be made using the amide I absorbance band.

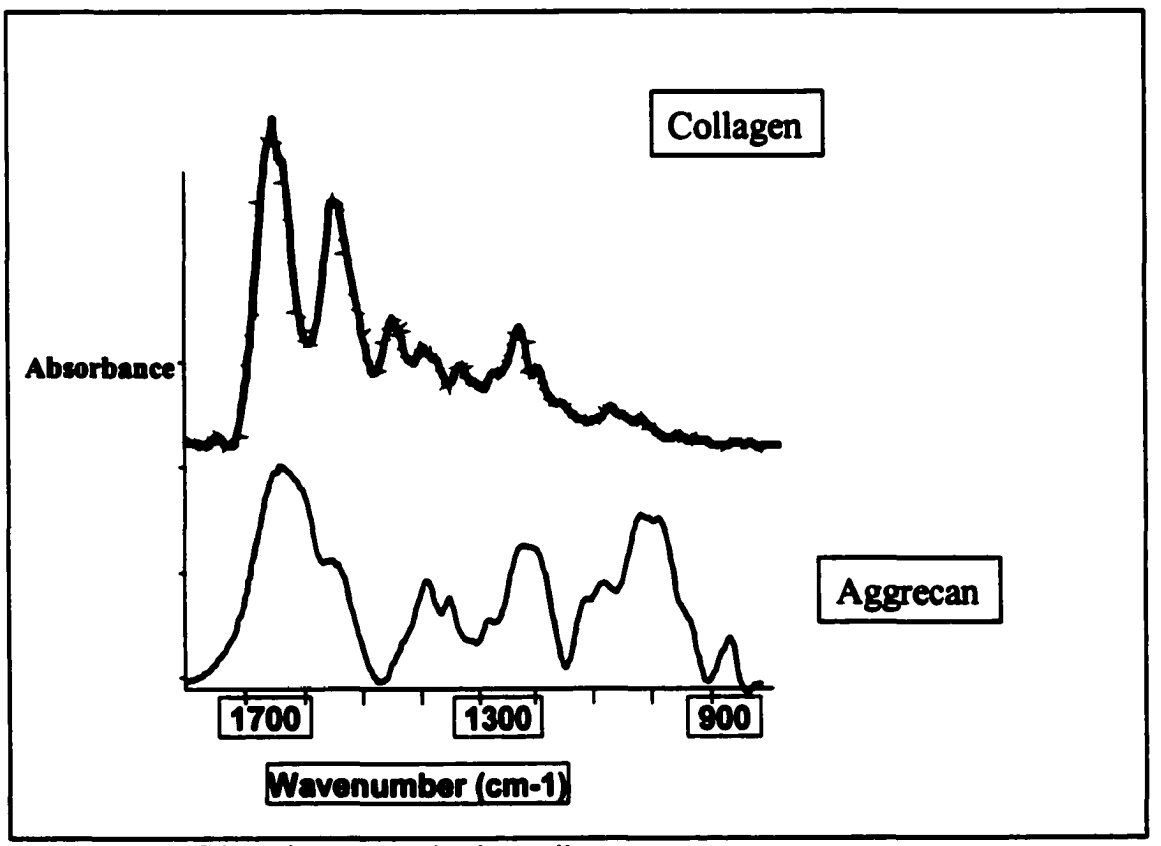

Fig. 2-3: IR spectra of the primary proteins in cartilage.

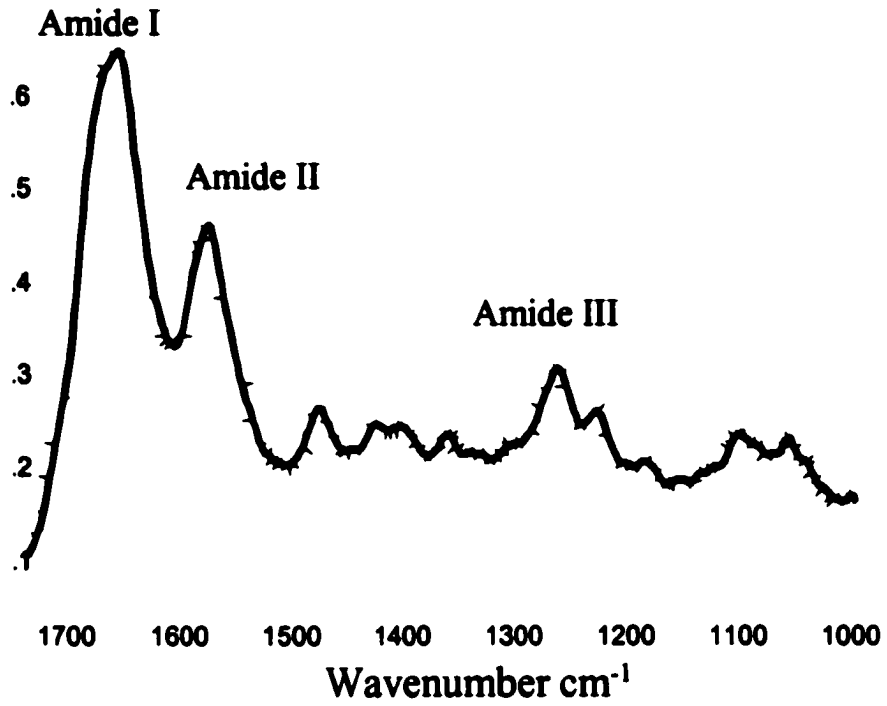

Fig. 2-4: IFOP spectrum of the articular surface.

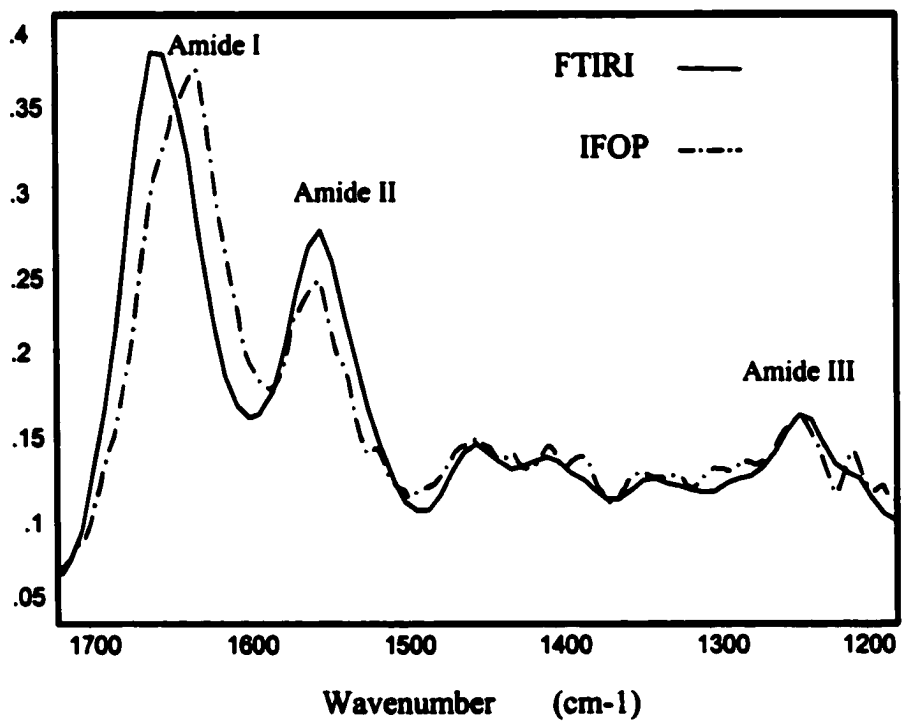

Fig. 2-5: Amide I band shift between FTIRI and IFOP.

Chapter III

FTIR Study of Model Compounds and Gels

Introduction

Articular cartilage biomechanical integrity depends primarily on its well-maintained proteoglycan to collagen ratio. An imbalance in this ratio usually signals the onset of disease. Therefore to identify spectral changes related to proteoglycan:collagen ratio changes, it is necessary to analyze mixtures of these two matrix compounds. In this study FTIR spectroscopy was used to analyze proteoglycan:collagen model compounds and aggrecan gel mixtures.

Materials and Methods

1. **Model Compounds**: Purified calf nasal aggrecan (Montefiore Hospital, Bronx, NY) and chick Type II collagen (Genzyme, Boston, MA) were mixed as model compounds and analyzed by FTIR as KBr pellets using a Mattson Cygnus 25 Infrared Spectrometer (Mattson Instruments, Madison, WI). Each sample set contained five KBr pellets of constant 2 mg sample size (2-mg sample, 200 mg KBr) in which the aggrecan percentage was varied in 25% increments from 0 – 100%. Eleven sets were made in all. Each sample set was then analyzed using transmission FTIR for spectral changes related to the incremental increases in the aggrecan to collagen weight ratio. Spectra were obtained using 256 scans at 4 cm^{-1} resolution.

2. **Gels**: A 40% stock solution of purified chick aggrecan (Sigma-Aldrich Co., USA) was made by adding 2-mgs of aggrecan to 5 ml of 0.15 mM tris buffered solution at a

pH of 7.4. The solution was continuously stirred in a 4 ^{0} C fridge for 5 days. Upon removal, different amounts of a 20% gelatin solution were added to produce 10, 20, and 30% aggrecan solutions. These solutions were placed overnight in a -70 ^{0} C freezer, then cryosectioned at 6 μm thickness and placed onto barium fluoride windows. Four sections were cut for each % mixture. The BioRad (Cambridge, MA) UMA 300A FTIR microscope with an FTS-60A step-scanning FTIR spectrometer and a 64x64 MCT FPA detector (Stingray Imaging Spectrometer) was used to acquire FT-IRI data for all the sections at 8 cm^{-1} resolution under N_2 purge. Information on aggrecan distribution was then obtained from a 400 x 400 μm^2 region, resulting in 4,096 individual spectra for each % sample group. Using the aggrecan (C-O-C) and amide I (C=O) absorbance bands, the PG/Amide I area ratio distribution was calculated for each % group using Grams/32 software (Galactic Industries, Salem, NH).

Results

Model Compounds: FTIR spectra of model compounds containing both 100% type II collagen and 100% aggrecan showed considerable overlap. The primary absorbance bands (peptide bond vibrations) in collagen are amide I, II, and III (Table 1), while for

Table 2: Infrared Frequencies of Collagen and Proteoglycan in Cartilage.

Bond Vibrations	Collagen	Proteoglycan(PG)
Amide I C=O stretch	1655 cm-1	1642 cm-1
Amide II C-N stretch, N-H bend combination	1550 cm-1	1560 cm-1
Amide III C-N stretch, N-H bend, C-C stretch/ Sulfate stretch (PG)	1240 cm-1	1240 cm-1
C-O-C, C-OH, C-C ring vibrations		1125, 1070, 1040, 1000, 950 cm-1

aggrecan its primary features arise from sulfate, sugar, and protein entities. Upon increasing the aggrecan to collagen ratio, several progressive changes were noted in the spectra of the collagen:aggrecan mixtures (Fig. 3-1). The amide I and amide II peaks shifted from ~1660 to 1643 cm^{-1} and from ~1550 to 1564 cm^{-1}, respectively (Fig. 3-2). In addition, we observed linear increases in the 960-1185 cm^{-1} aggrecan absorbance region (Fig. 3-3), and linear decreases in the areas of the amide I (1710-1595 cm^{-1}), (Fig. 3-4) and the collagen 1338 cm^{-1} absorbance bands (Fig. 3-5).

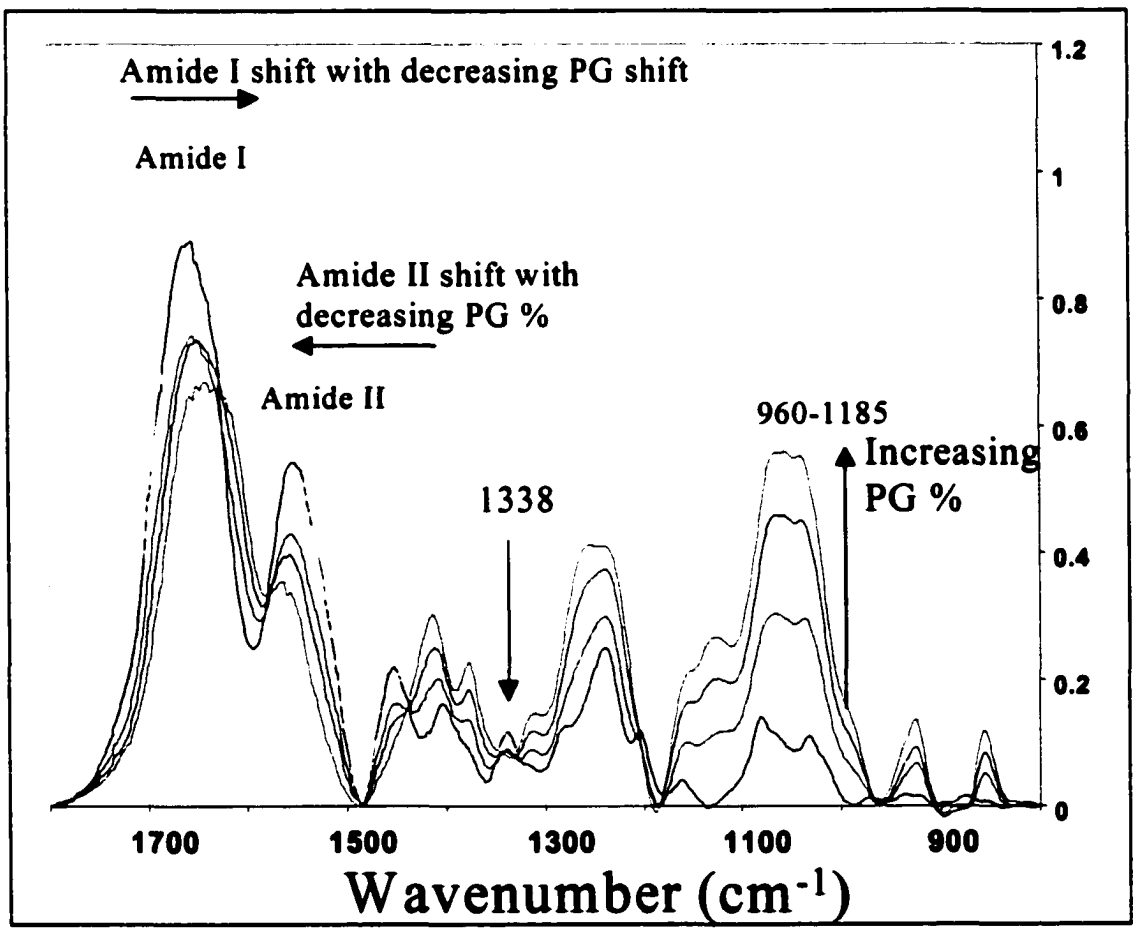

Figure 3-1: FTIR spectra from KBr pellets of mixtures of type II collagen and aggrecan.

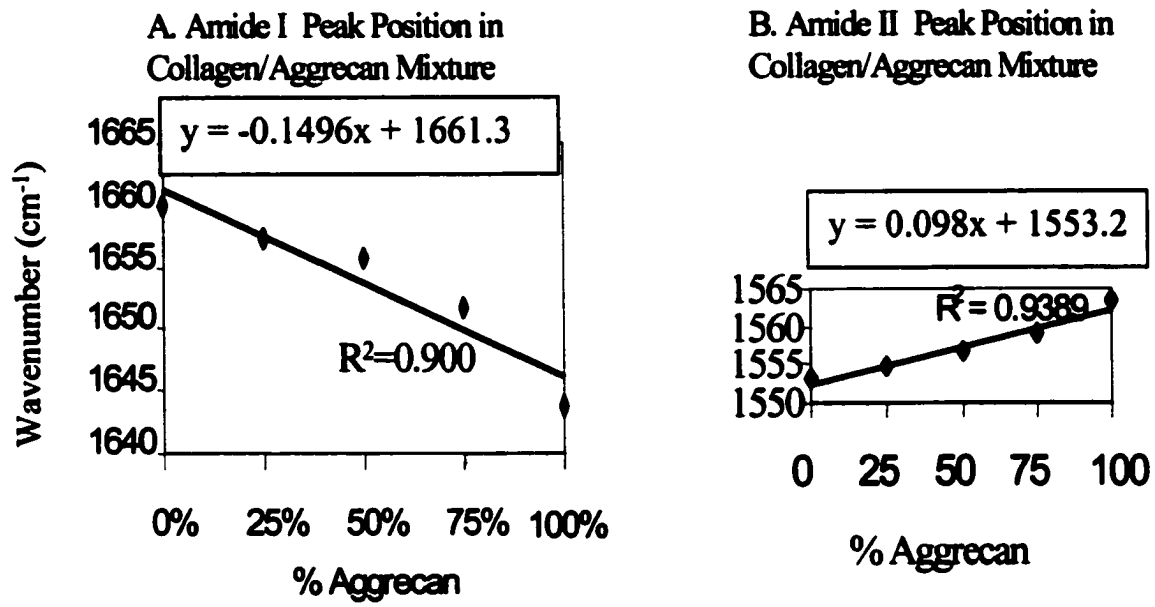

Fig. 3-2: (A) Amide I peak position shift vs. % aggrecan. (B) Amide II peak position shift vs. % aggrecan.

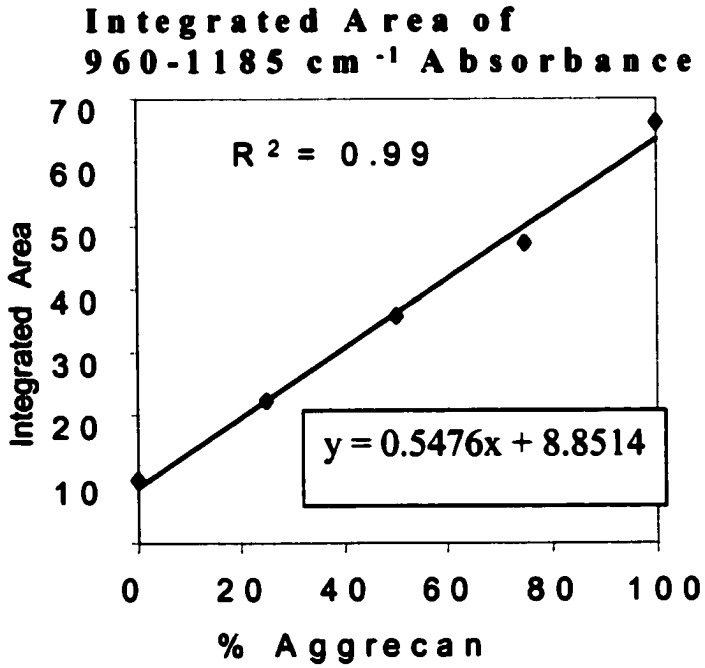

Fig. 3-3: Integrated area of 960-1185 cm^{-1} peak vs. % aggrecan.

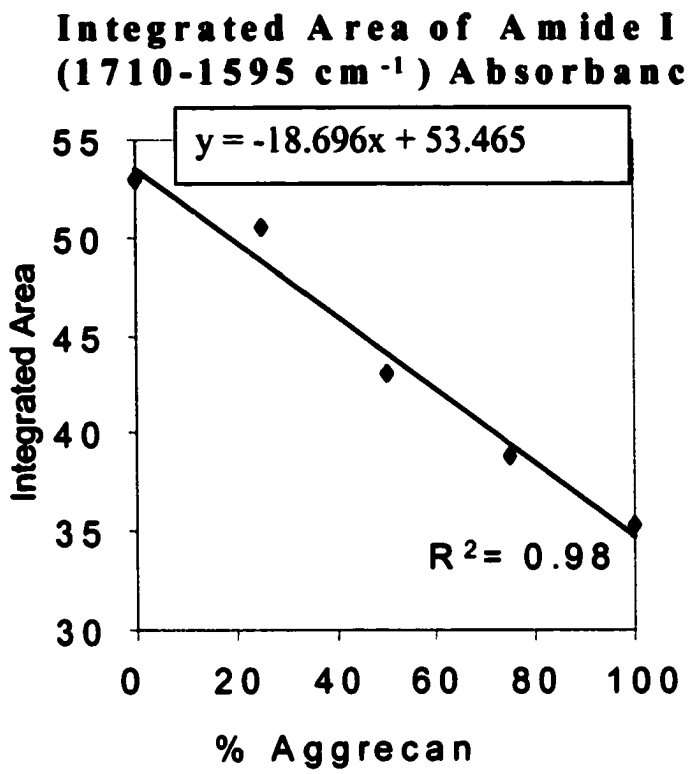

Fig. 3-4: Amide I collagen peak (1710-1585 cm^{-1}) vs. % aggrecan.

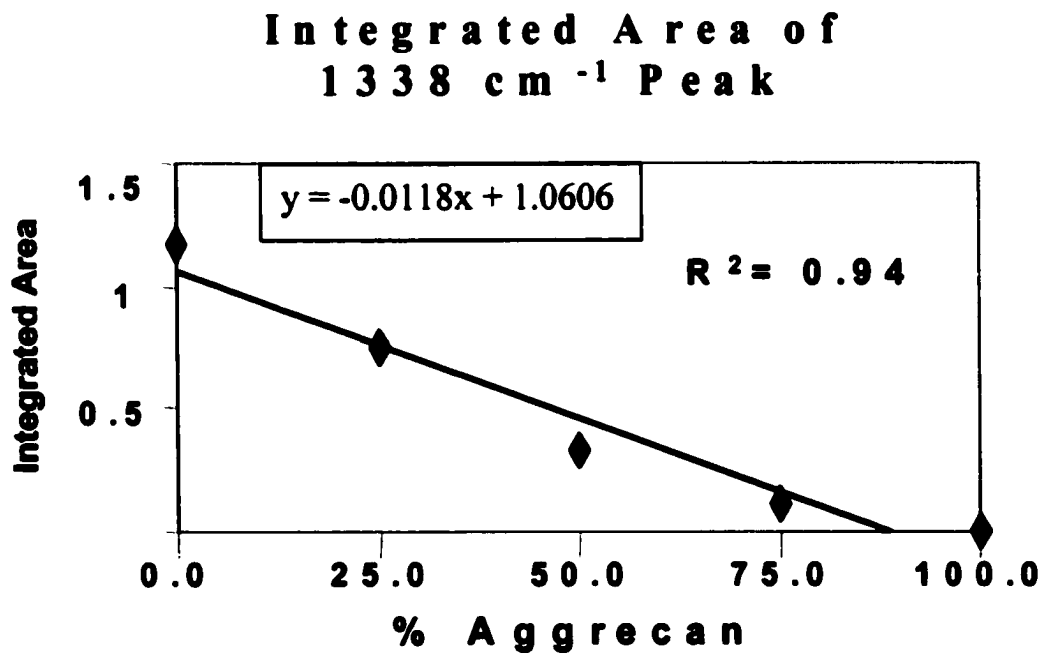

Fig. 3-5: 1338 cm^{-1} collagen peak vs. % aggrecan.

Gels: The aggrecan (PG) absorbance bands (sugar ring vibrations) showed good corelation with the different % mixtures. FTIR spectra of 0,10,20, and 30% aggrecan gel mixtures showed progressive increases in the PG/amide I absorbance ratio (fig. 3-6). Upon increasing the aggrecan percentage, we observed linear increases in the PG/amide I absorbance ratio (fig. 3-7). These findings were also correlated with the 25% KBr model compound mixtures (fig. 3-8).

Fig. 3-6: Illustration of the amide I and aggrecan (PG) integrated areas.

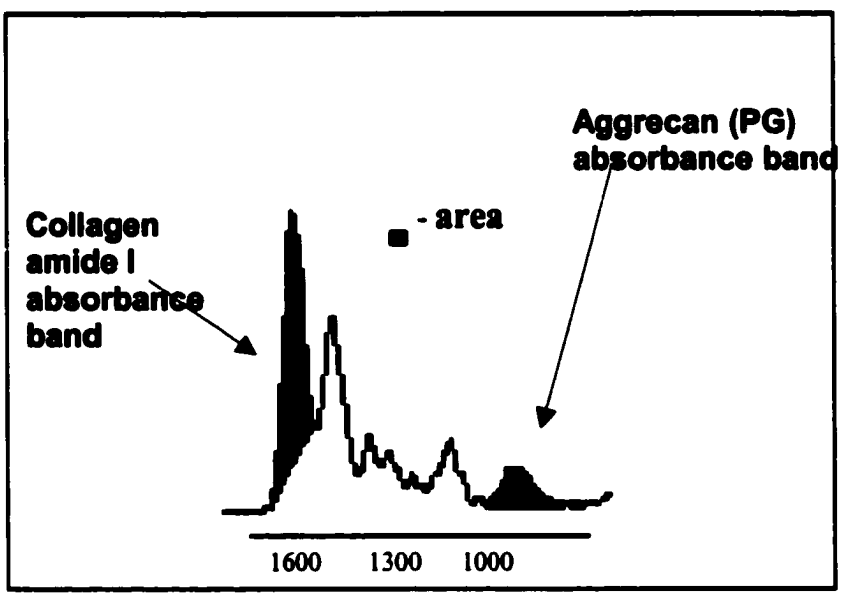

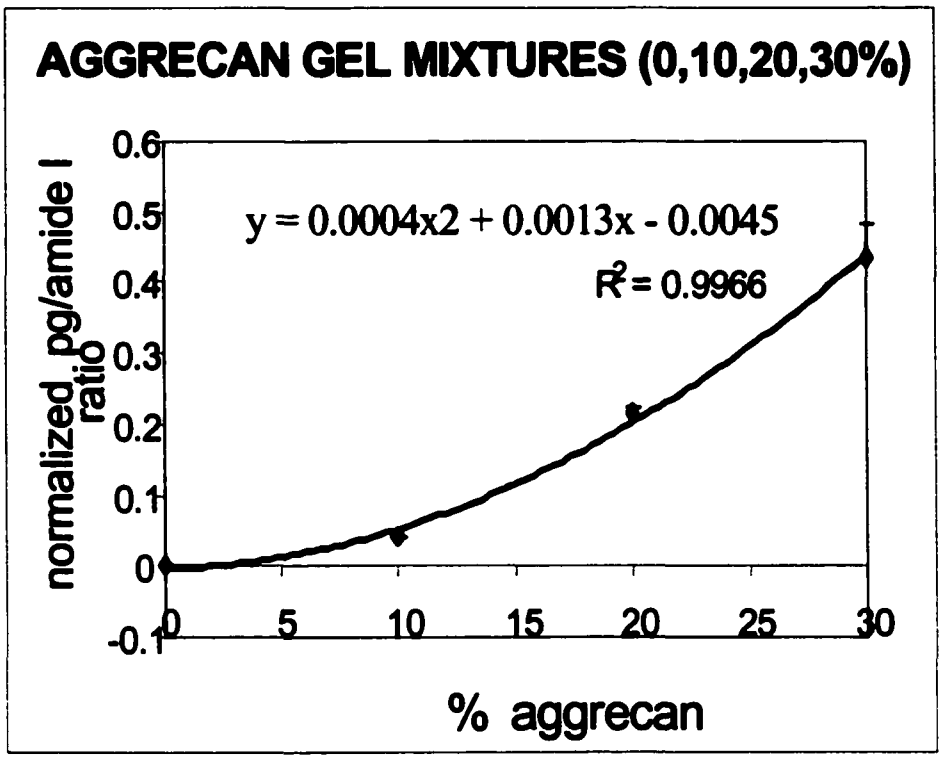

Fig. 3-7: Normalized PG/amide I ratio vs. % aggrecan

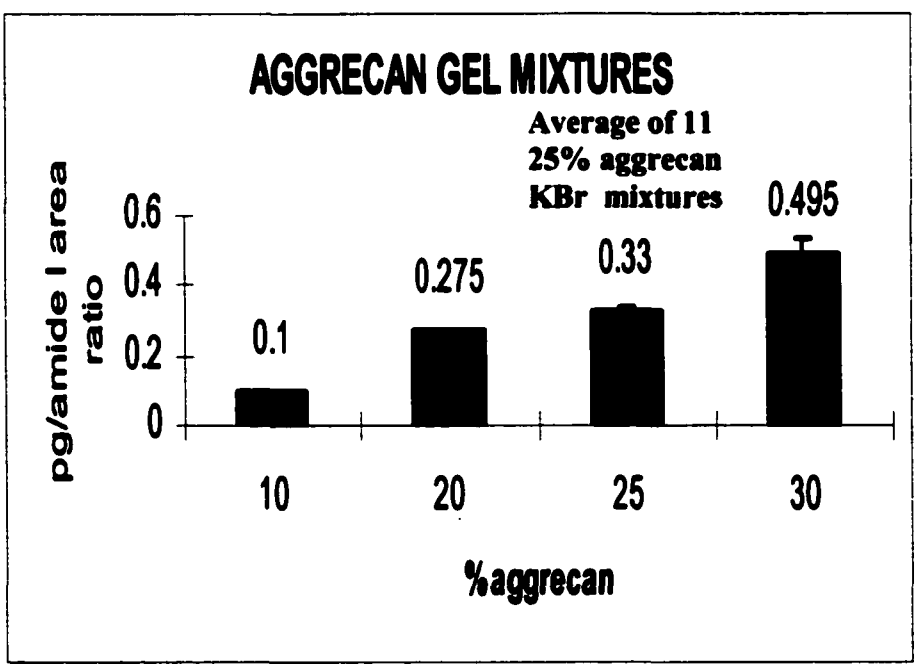

Fig. 3-8: PG/amide I comparison between gel mixtures and KBr model compounds.

Discussion

In this study, spectral absorbances were identified that arise from the primary constituents of articular cartilage, namely type II collagen and proteoglycan. For both model compounds and gels, changes in type II collagen or proteoglycan composition resulted in changes in specific IR absorbances. Higher type II collagen composition typically resulted in higher amide I (1710-1595 cm^{-1}) and peak 1338 absorbances, while higher PG composition resulted in a higher IR absorbance in the 960-1185 cm^{-1} peak area. More important however, in comparing the PG/amide I IR parameter between the model compounds and the gels (Fig. 3-8), we see that the average of the eleven 25% PG (aggrecan) KBr mixtures fits nicely between the values of the 20% and 30% aggrecan gel mixtures. This implies that the prediction plot (Fig. 3-7) generated by the gel mixtures may provide a good estimate based on PG/amide I area ratio of the percentage proteoglycan in articular cartilage samples.

This new application of IR technology may prove potentially useful for the detection of compositional changes within articular cartilage that occur as a result of disease or mechanical damage. The onset of early osteoarthritis is accompanied by early molecular changes, such as collagen or proteoglycan breakdown, that potentially lead to changes in the PG:collagen ratio. These early stage changes that involve breakdown of matrix molecules but no obvious mechanical damage are much more difficult to identify using conventional techniques. The use of FTIR spectroscopy in the identification of these changes will provide significant insight into the mechanism of early articular cartilage degradation.

Chapter IV

FTIR Evaluation of Genetically Modified Bovine Chondrocytes

Introduction

Recent advances in tissue engineering have led to the development of synthetic cartilage tissue (Carticel-Genzyme Biosurgery) for implantation into chondral defects. Autologous cultured chondrocytes (Carticel®) developed from the culture of a patient's own (autologous) cartilage cells, is used in the repair of cartilage defects of the femoral condyle. Currently there are no available methods for assessing the integrity of tissue engineered matrix macromolecules at the ultrastructural level before and after implantation. Tools to assess the integration and regeneration of the tissue engineered matrix molecules with that of the native cartilage are also needed.

In this study, FTIR Imaging is used to evaluate compositional changes in genetically modified bovine chondrocytes.

Materials and Methods

These procedures were done by Dr. Hidaka in the Laboratory for Soft Tissue Research at the Hospital for Special Surgery.

Fresh 6-mm diameter cartilage explants were harvested from mature bovine occipital articular cartilage strips. Bovine chondrocytes were then isolated by overnight digestion using a 0.1% bacterial collagenase solution (Gibco, Grand Island, NY). After digestion, the chondrocytes were maintained in a growth media consisting of 10% fetal bovine serum (FBS), 100 U/ml penicillin, 100mg/ml streptomycin (all from Gibco) and 1% Fungizone

(Biofluids, Rockville, MD). The chondrocytes were later infected with 5000 particle units (pu)/cell of adenovirus (Ad) vectors AdBMP-7, Adβgal, or no virus (naive) for 2 hours on a rocker at 37° C. Infected chondrocytes were transplanted onto the cut surface of cartilage explants for 1 hour in a humidified atmosphere at 37° C before submerging in additional growth media supplemented with 50 μg/ml ascorbate (Sigma, St Louis, MO). For each tissue, a paraffin-embedded 6-μm section was cut directly onto a BaF_2 window and examined by FTIR Imaging. Xylene was used to dissolve the paraffin, and the section air-dried before analysis. The BioRad (Cambridge, MA) UMA 300A FTIR microscope with an FTS-60A step-scanning FTIR spectrometer and a 64x64 MCT FPA detector (Stingray Imaging Spectrometer) was used to acquire spectra at 8 cm^{-1} resolution under N_2 purge. Data were collected from a 400 x 400 μm^2 region mapped to the individual elements of the array detector, resulting in 4,096 individual spectra.

Imaging data were analyzed with WinIR Pro software (BioRad), while histograms were created using Origin software (Microcal Software, Northampton, MA). Information on the integration of the newly formed matrix (via transfected chondrocytes) into the articular cartilage explant was based on the integration areas of the amides I (1655 cm^{-1}) and II (1550 cm^{-1}) collagen absorbance and on the proteoglycan sugar peaks (960-1185 cm^{-1}). IR images were also created based on the integrated areas of the amide I absorbance and on the proteoglycan sugar absorbance to (amide I + amide II) area ratio. Amide I images showed collagen distribution, while the PG/(amide I + amide II) images showed relative quantity and distribution of the proteoglycan component. Histograms were created from each image to show the distribution of absorbance values in the tissue, and means ± standard deviations were reported.

Results

FT-IR Imaging was used to generate tissue images based on collagen (Fig. 4-1A-C) and proteoglycan (Fig. 4-2A-C) content. For all the sections analyzed, a distinct interface was observed between the bovine articular cartilage and the transplanted bovine chondrocytes. IR Imaging analysis showed that the AdβMP-7 treated chondrocyte matrix appeared to produce more proteoglycan compared to both Adβgal-treated and naïve chondocyte matrix, and to native bovine articular cartilage. This was also confirmed both statistically (see histogram Fig. 4-2D-F) were the average values for proteoglycan content was higher than that of the naïve and Adβgal controls and also by mRNA analysis (24) which showed a five-fold increase in proteoglycan in the AdβMP-7 treated chondrocytes compared to the naïve chondrocytes. In addition, the IR imaging data showed that the distribution of the proteoglycan component in the AdβMP-7 chondrocyte matrix was more heterogeneous than either the naïve or Adβgal-treated chondocyte matrix. There were only moderate differences (Fig. 4-1D-F) in collagen distribution.

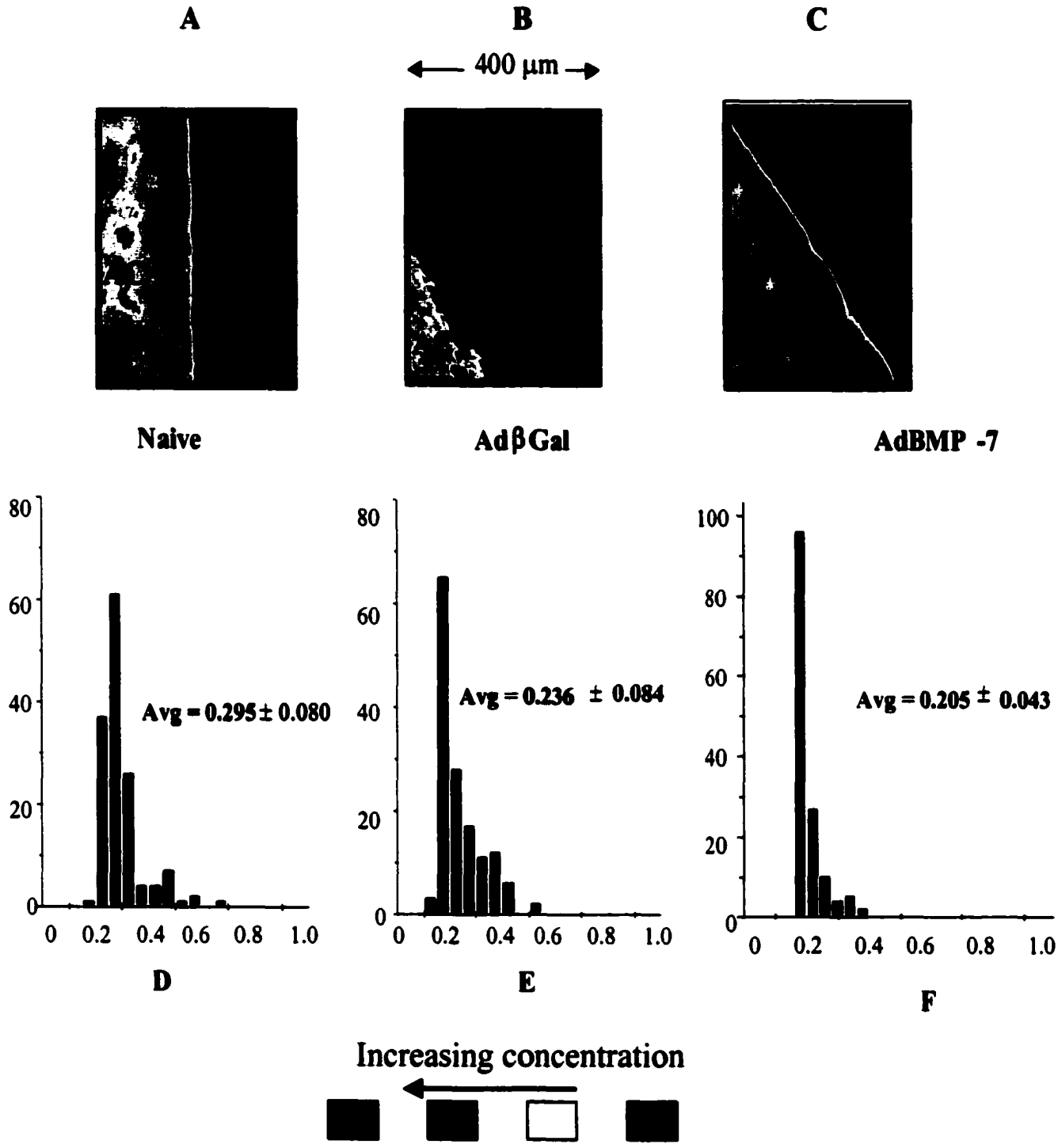

Fig. 4-1: (A-C) - FTIR images (amide I peak area) of articular cartilage (AC) with transfected bovine chondrocytes (BC) . (D-F) – Histograms of the normalized amide I peak area for naïve (D), Adbgal(E) and AdBMP-7 (F) treated repair tissue.

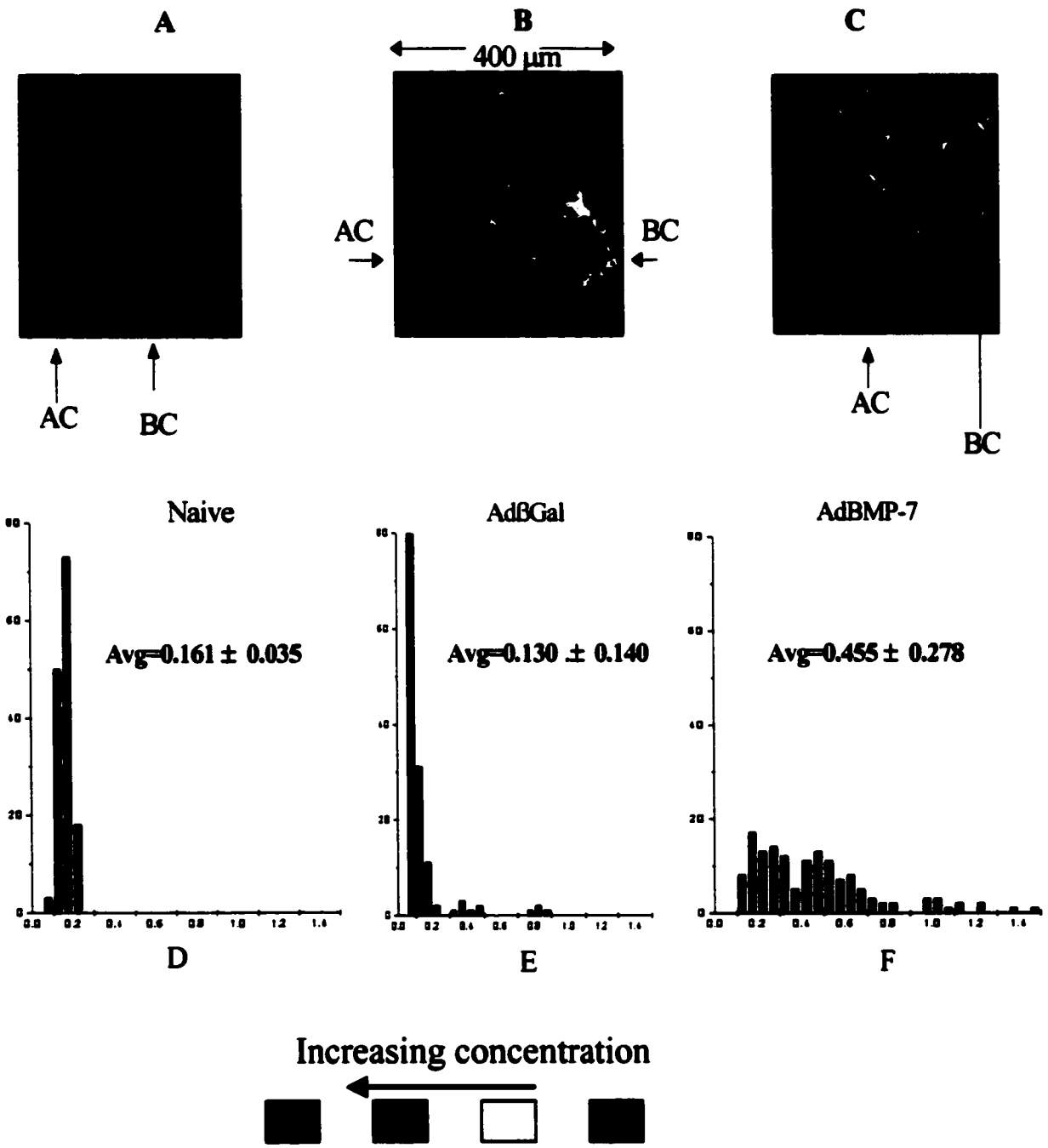

Fig. 4-2: (A-C) - FTIR images based on proteoglycan (960-1185 cm^{-1})/amide I & II absorbance area) of articular cartilage (AC) with transfected bovine chondrocytes (BC) . (D-F) – Histograms for this peak ratio (proteoglycan (960-1185 cm^{-1})/amide I & II absorbance) for naïve (D), Adbgal(E) and AdBMP-7 (F) treated repair tissue.

Discussion

In this study, FT-IR imaging was used for visualization and quantitation of the components of repair tissues in an in vitro model of gene-modified autologous chondrocyte transplantation. Compared to standard histological methods, which showed the presence of proteoglycan in the tissue formed by naïve, Adβgal and AdBMP-7 treated chondrocytes, quantitation by FT-IRI revealed that the AdBMP-7 treated group contained the highest amount of proteoglycan. This increase in the proteoglycan content was consistent with our previous findings of a five-fold increase in aggrecan gene expression by AdBMP-7 treated chondrocytes (24). FT-IRI analysis also showed a moderate decrease in the type II collagen content in the AdBMP-7 treated group when compared to both the controls and the native cartilage. This result conflicts with our findings of increased type II collagen gene expression in a previous study. On the other hand, immunohistochemistry simply showed the presence of type II collagen in the tissues formed by all groups of chondrocytes.

BMP-7 is an important limb forming growth factor which is expressed in normal articular cartilage (25-29). Previous studies have shown that stimulation of chondrocytes by BMP-7 whether by incubation with recombinant proteins or genetic modification can enhance matrix production (30-32). Compared to these previous studies which have examined the BMP-7- stimulated synthesis of both proteoglycan and type II collagen, our use of FT-IRI enables us to show the proportions of the two matrix components produced by BMP-7 expressing cells, and to compare them to that of native cartilage. Our results show that BMP-7 preferentially enhances proteoglycan matrix deposition over that of collagen. Increased proteoglycan content in cartilage has been shown to correlate with increased compressive strength. These findings suggest the potential for forming engineered cartilage

tissue with enhanced compressive strength by using AdBmp-7- modified chondrocytes. However, since the physiology of articular cartilage requires a balance in matrix proteins, an alternate strategy, which enhances type II collagen deposition, will be required.

In this study we show the importance of quantitating matrix components: type II collagen and proteoglycan at the protein level, as opposed to the nucleic level, when assessing tissue formation.

CHAPTER V

Development of the Infrared Fiber Optic Sampling Methodology

Introduction

The goal of this study is to investigate and develop Infrared Fiber Optic Probe (IFOP) sampling methodology that will produce accurate and reproducible IR data with negligible tissue damage. An ATR crystal equipped FTIR fiber optic probe will be designed for the acquisition of IR data from the surface of articular cartilage, where molecular information on surface proteins can be obtained. Due to the intrinsic nature of ATR technology, where light penetration depth (P_d) into the sample is on the order of λ, good surface contact between sample and crystal is essential. Good surface contact however, requires pressing on the sample, which may ultimately lead to mechanical damage. In this study we investigate two different ATR crystal tip designs within the context of tissue damage and IR spectral quality. The questions to be addressed are:

a) What is the minimum distance the tissue can be displaced in order to have good surface contact and reproducible spectra?

b) Is there resultant mechanical damage?

An initial zinc selenide (ZnSe) conical shaped ATR tip (Fig 5-1A-(2 bounce system)) and a redesigned zinc sulfide FDA approved (ZnS) flat ATR tip (Fig.5-1B- (3 bounce system)) will be investigated.

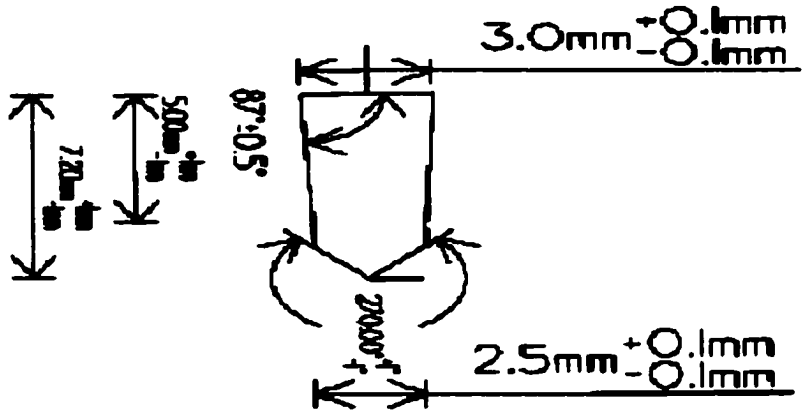

Fig.5-1A: ZnSe conical ATR tip

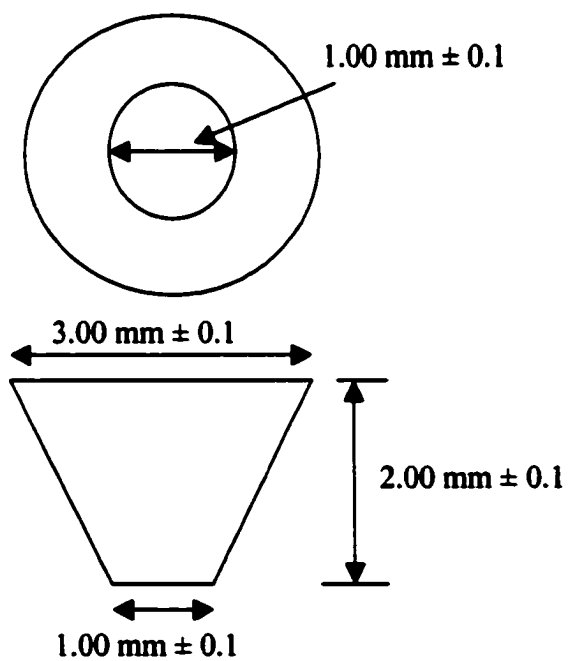

Fig. 5-1B: ZnS ATR flat probe tip.

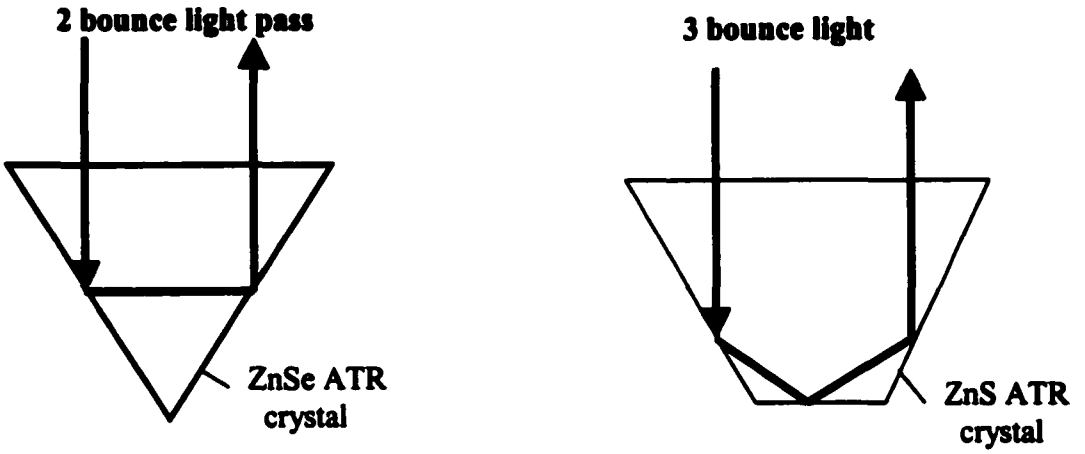

Fig. 5-1C: Schematic of 2 and 3 bounce light pass in ATR crystal .

Materials and Methods

Infrared Fiber Optic Probe (IFOP): The Infrared Fiber Optic Probe consists of a flexible fiber optic bundle composed of a mid-infrared transmitting "chalcogenide" glass (RemSpec Corp, Sturbridge, MA) equipped with an Mercury Cadmium Telluride (MCT) detector module coupled to a BRUKER spectrometer (BRUKER, Germany). Chalcogenide glass is transparent to mid-infrared radiation and is made with the addition of the chalcogen elements (sulphur, selenium and tellurium). The fiber optic bundle is approximately 1 meter in length and transmissive over the infrared region of 4000 - 900 cm^{-1}. IR sampling is achieved by the use of an ATR (attenuated total reflectance) crystal attached to the end of the fiber optic bundle.

IFOP Sampling Methodology: The fiber optic probe was gently pressed on intact, 5 mm diameter articular cartilage explant plugs that were secured on a 10 μm resolution micrometer driven Z stage on which initial ATR tip contact, and subsequent force/displacement can be measured. Infrared data on extracellular matrix content,

distribution, and integrity was then acquired from the surface using ATR spectroscopy. All sampling was done under unconfined compression in a wet bath, after samples had been stored overnight in phosphate buffered saline (PBS) at 4 ^{0}C.

To optimize surface and optical contact, sampling at different displacement depths was investigated. With incremental increases in applied force, each specimen was sampled to different displacement depths. At each depth, an IR spectrum was taken after the tissue was allowed to relax for 10 minutes. The data collected was then averaged and correlated to changes in the spectrum signal-to-noise ratio. Sampling time was 1 minute (212 scans/sample at a 4 cm^{-1} wavenumber resolution).

After sampling, tissues were separated into two groups. One group was fixed in formalin and its surface morphology evaluated using scanning electron microscopy (SEM). The remaining group was analyzed for cell viability (Paravital stain) in order to ascertain if there was an effect from the indentation of the probe tip. Paravital stain is a fluorescence-based method used for determining cell viability. Two biological probes: calcein AM and ethidium homodimer-1 are used. Calcein AM (membrane-permeant) is cleaved by esterases in live cells to yield cytoplasmic green fluorescence, while ethidium homodimer-1 (membrane-impermeant) labels nucleic acids of dead cells red. Staining was observed using a fluorescent microscope (10x). Filter wavelength was 495 nm.

ZnSe conical ATR probe tip: IR sampling at different displacement depths was investigated on 10 normal immature bovine articular cartilage specimens. All samples were cut to a 5mm thickness. After initial contact, each specimen was sampled to five successive displacements, .5mm, .75mm, 1mm, 1.25mm and 1.5mm respectively.

ZnS flat ATR probe tip: IR sampling at different displacement depths was investigated on 6 normal articular cartilage specimens: 3 mature bovine and 3 mature human. Measured cartilage thickness for the bovine and human sample was 910 μm and 2050 μm, respectively. After initial tip contact, each specimen was sampled to six successive displacements 50 μm apart (50,100,150,200,250,300 μm).

Results

ZnSe conical ATR probe tip: The IR spectra obtained revealed a direct proportionality between displacement and the signal-to-noise ratio, where deeper displacements resulted in better quality spectra. Changes in the amide absorbance areas showed linear increases with tip displacement (Fig. 5-2A), due to the subsequent increase in the contact surface area of the ATR crystal (Fig. 5-2B). However, when amide absorbances were ratioed and averaged, significant changes were no longer observed after a tip displacement of ~1.25mm (Fig. 5-3).

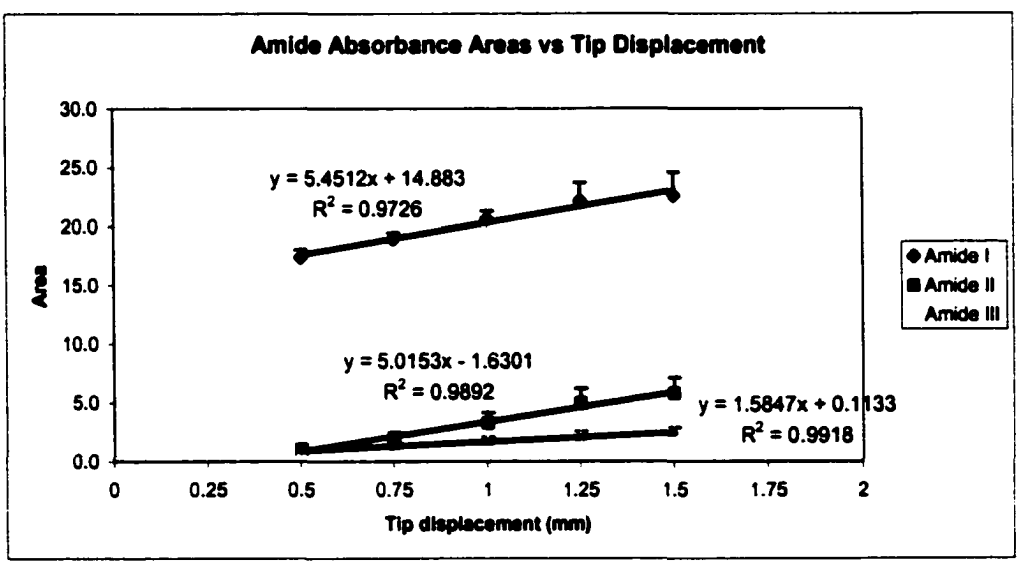

tip	amide I area		amide II area		amide III area	
displ(mm)	Mean	STD	Mean	STD	Mean	STD
0.50	17.38	0.64	1.00	0.45	0.86	0.25
0.75	18.95	0.52	1.94	0.53	1.31	0.30
1.00	20.61	0.66	3.27	0.87	1.78	0.28
1.25	22.13	1.55	4.94	1.27	2.11	0.43
1.50	22.60	1.98	5.77	1.35	2.43	0.45

A

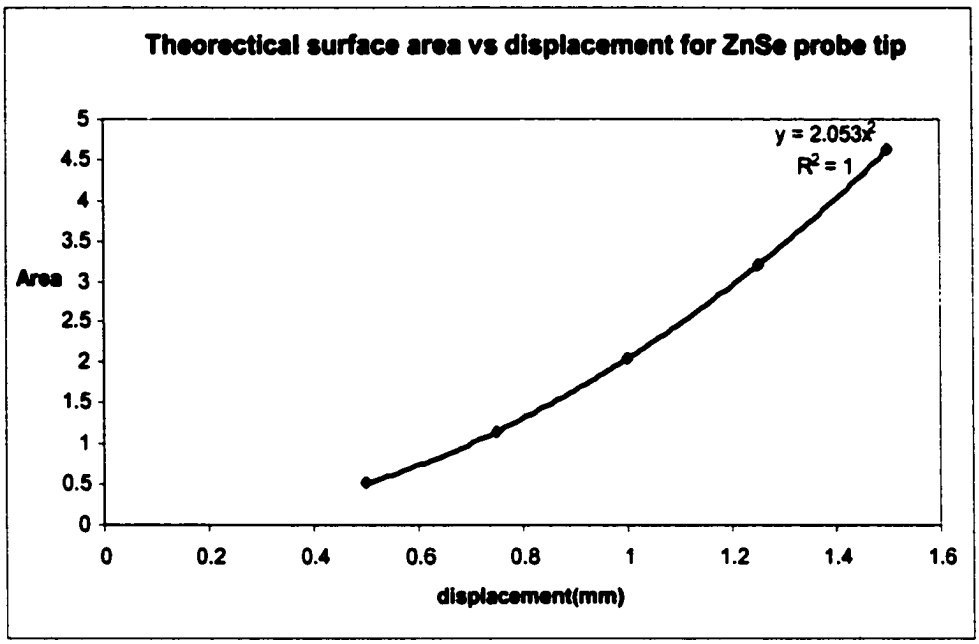

B

Fig. 5-2: A: Amide absorbances vs. ZnSe conical ATR tip displacement.
B: Theoretical surface area vs. displacement for conical ZnSe ATR tip.

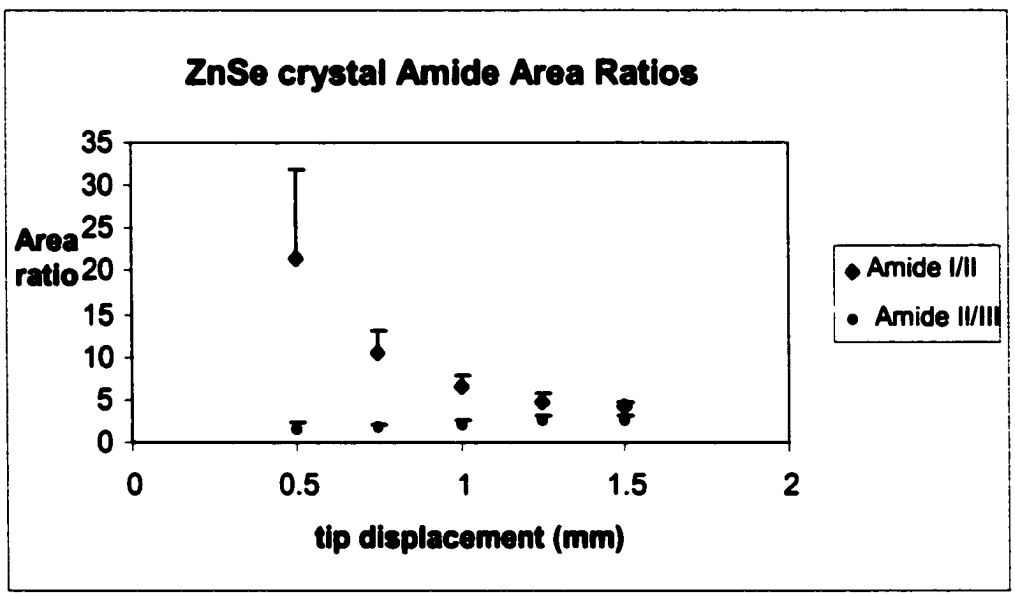

tip (mm)	Amide I/II area	
displ	Mean	STD
0.5	21.348	10.39331
0.75	10.4133	2.77122
1	6.6044	1.3362
1.25	4.6923	0.98566
1.5	4.0654	0.736219

tip (mm)	Amide II/III area	
displ	Mean	STD
0.5	1.627254	0.649933
0.75	1.761243	0.421357
1	2.043297	0.513985
1.25	2.60792	0.560645
1.5	2.618356	0.536796

A

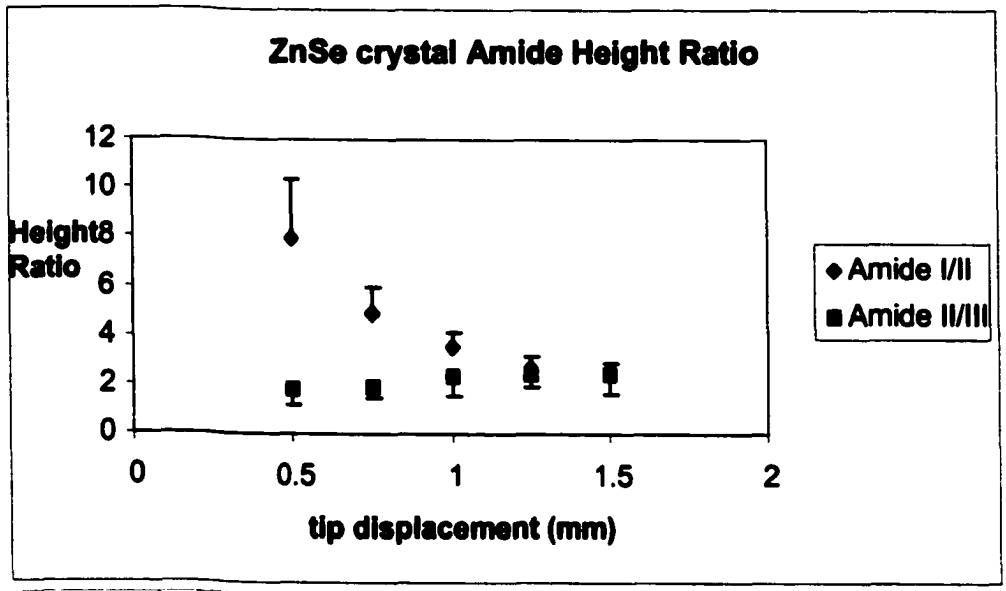

Tip (mm) displ	Amide I/II Height Mean	STD
0.5	7.9084	2.438767
0.75	4.8533	1.125442
1	3.4869	0.7
1.25	2.7466	0.4359
1.5	2.5452	0.352485

Tip (mm) displ	Amide II/III Height Mean	STD
0.5	1.769148	0.554565
0.75	1.919994	0.51461
1	2.30487	0.754207
1.25	2.460731	0.603209
1.5	2.459663	0.812613

B

Fig. 5-3: (A) Amide area and (B) Height ratio variation vs. ZnSe probe tip displacement.

Morphological Assessment @ 1.25mm Tip Displacement: There were visible signs of damage at the articular surface. SEM evaluation of the articular surface revealed substantial damage created by the indentation of the ATR conical tip during IR sampling at ~ 1.25 mm. A relatively large hole (~ 1mm diameter) with tissue tearing at the bottom was observed microscopically (70 X- Fig. 5-4). Cell viability assessment at the indentation site using Paravital staining also revealed substantial damage. All the cells in the immediate vicinity of the sampling area had undergone necrosis (Fig. 5-5).

Fig. 5-4: Indentation on articular surface created by conical probe tip (mag: =70 x).

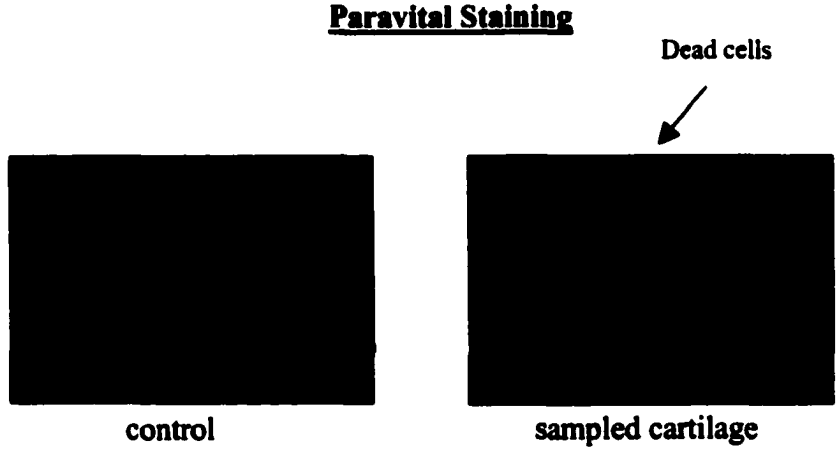

Fig. 5-5: Paravital staining showing cell death due to tip indentation.

ZnS flat ATR probe tip: The IR spectral quality revealed a similar direct proportionality between displacement and the signal-to-noise ratio, where deeper displacements resulted in higher spectral quality. Changes in the amide absorbance areas showed increases with tip displacement, due to the subsequent increase in the contact surface area of the ATR crystal (Fig.5-6). However, when amide II and III absorbances were ratioed for each type of cartilage, significant changes were no longer observed after a tip displacement of ~ 50 μm (Fig.5-7).

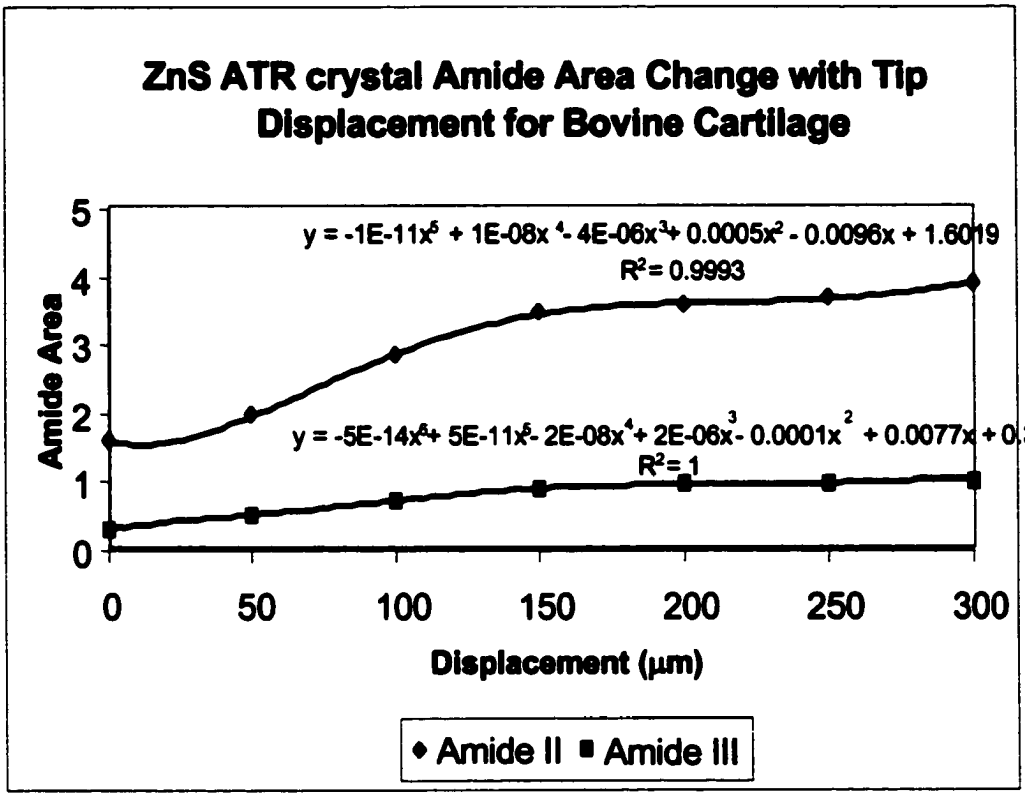

A

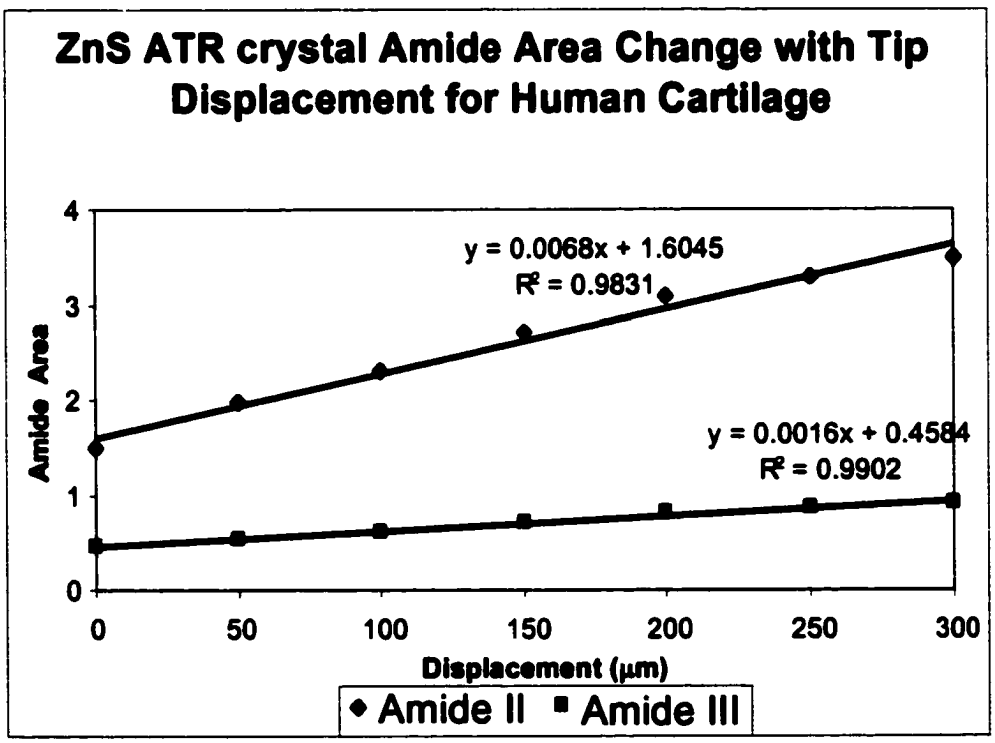

B

Fig. 5-6: Amide area variation vs. ZnS probe tip displacement for (A) Bovine and (B) Human cartilage.

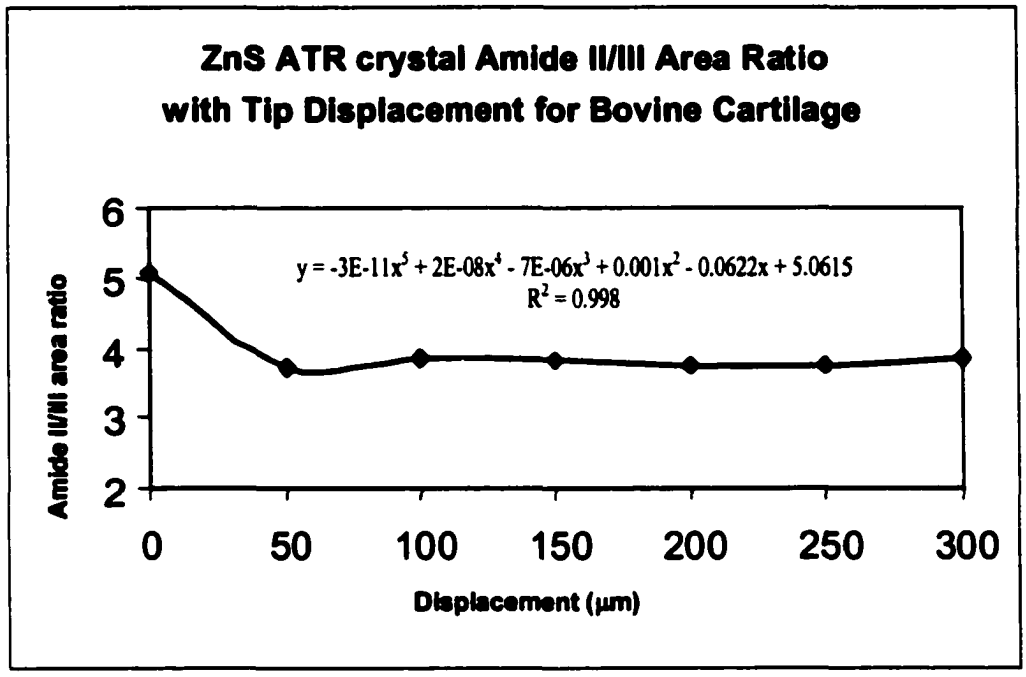

A

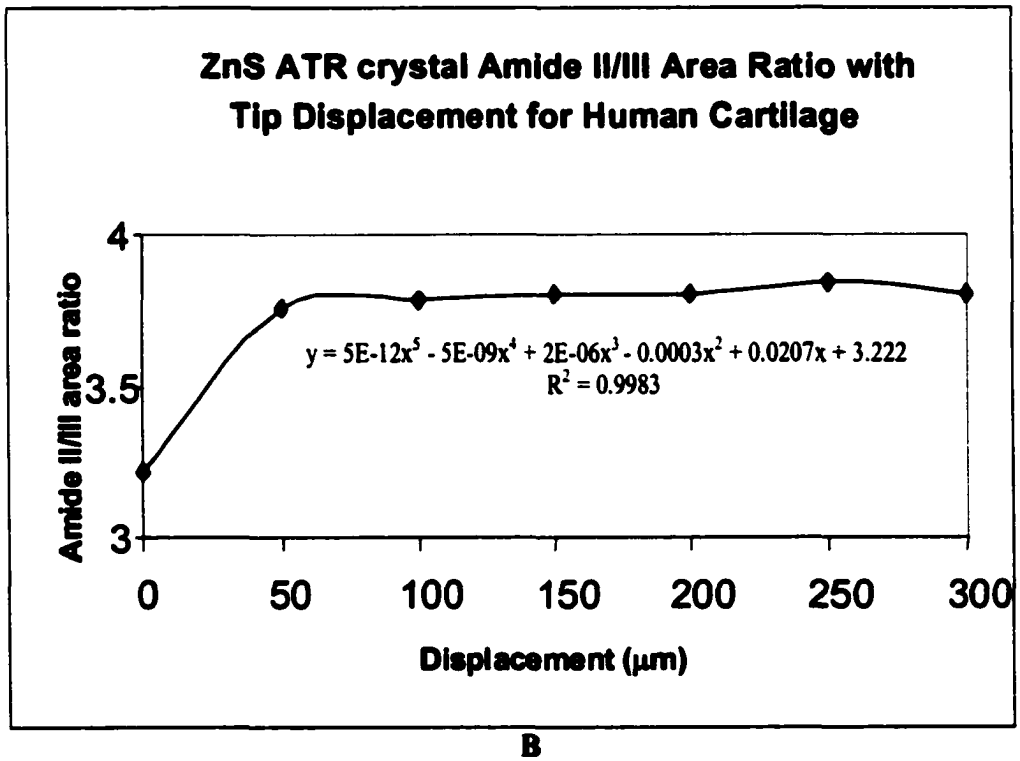

B

Fig. 5-7: Amide II/III area ratio variation vs. ZnS probe tip displacement for (A) Bovine and (B) Human cartilage.

Morphological Assessment @ 50 μm Tip Displacement: There were no visible signs of damage at the articular surface. Cell viability assessment at the sample site using Paravital staining revealed negligible cell death. A large majority of the cells in the immediate vicinity of the sampling area remained viable (Fig. 5-8). A SEM evaluation of the articular surface was not performed due to the lack of substantial cell death.

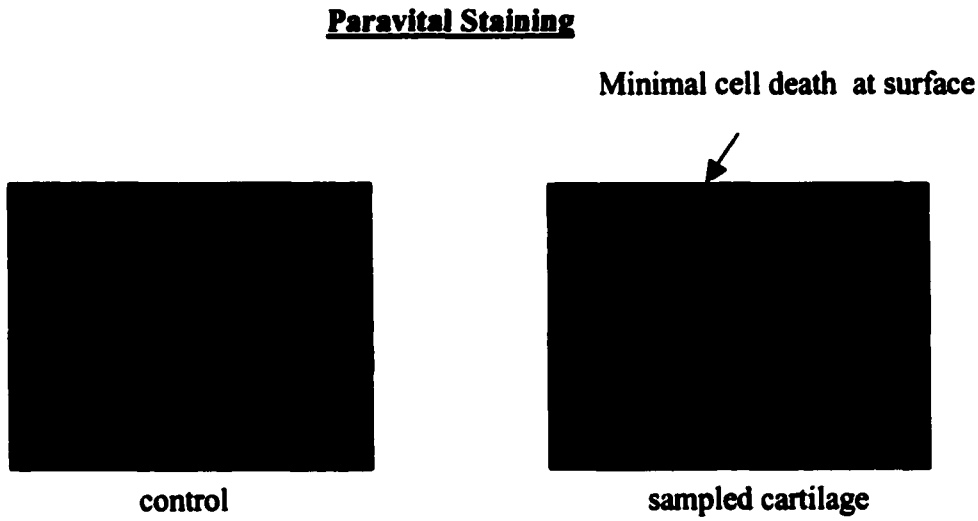

Fig. 5-8: Cell viability study @ 50 μm using the flat ATR probe tip.

Discussion

The objective of this study was to investigate and develop an Infrared Fiber Optic Probe (IFOP) sampling methodology that would produce accurate and reproducible IR data with negligible tissue damage. Investigation of our initial ZnSe conical ATR crystal resulted in large tip displacements for good optical contact with substantial damage to the articular surface, while the redesigned flat-tipped ZnS ATR crystal resulted in much smaller displacements with negligible damage. The flat-tipped ZnS ATR crystal also had

better signal-noise-ratio because of its three-bounce light pass system (more bounces or reflections = higher signal-noise-ratio). Our results clearly show that the flat-tipped ZnS ATR crystal is better suited for diagnostic purposes. A spherical ATR crystal tip was also considered, however, due to uncertainty in determining the light path within the crystal and machining complications, it was not pursued.

CHAPTER VI

Observing the Effects of Stress Relaxation on the IFOP Spectral Quality

Introduction

Biomechanically, articular cartilage is considered a biphasic material consisting of a solid matrix (~30%) and a fluid phase (~70%). It is essentially a swollen, shock absorbing fiber-reinforced solid matrix in which the tensile/reinforcement properties come from the collagen fibrils, while the swelling properties are due to the very hydrophilic sequestered proteogylcans. This contributes to its viscoelastic nature, thus when it is deformed and held at constant strain, it undergoes stress relaxation (Fig. 6-1). Viscoelasticity is defined as the time-dependent behavior a material exhibits whenever it is subjected to a constant load or constant deformation. This viscoelasticity in cartilage is primarily a flow-dependent phenomenon caused by pressurization within the tissue, followed by fluid flow through the porous solid matrix and energy dissipation. *In vivo*, it is this feature of cartilage that makes it capable of withstanding high compressive loads.

From the work in the previous chapter, it was decided that the FDA approved ZnS ATR crystal was better suited for medical diagnostics, largely because of its flat tipped geometry which provided good surface contact (50-100μm displacement range) without substantial tissue damage. However, in light of the viscoelastic properties of cartilage there are some questions that need to be addressed:

a) what is the minimum time contact needs to be maintained with the probe on the articular surface at a 50μm depth before data is acquired?

b) what are the time-dependent effects of free water movement (matrix compaction) on spectral quality during sampling?

c) are the acquired IR spectra sensitive to the effects of compression on water trapped (bound) within the collagen fibrils?

These are the questions that will be investigated in this chapter.

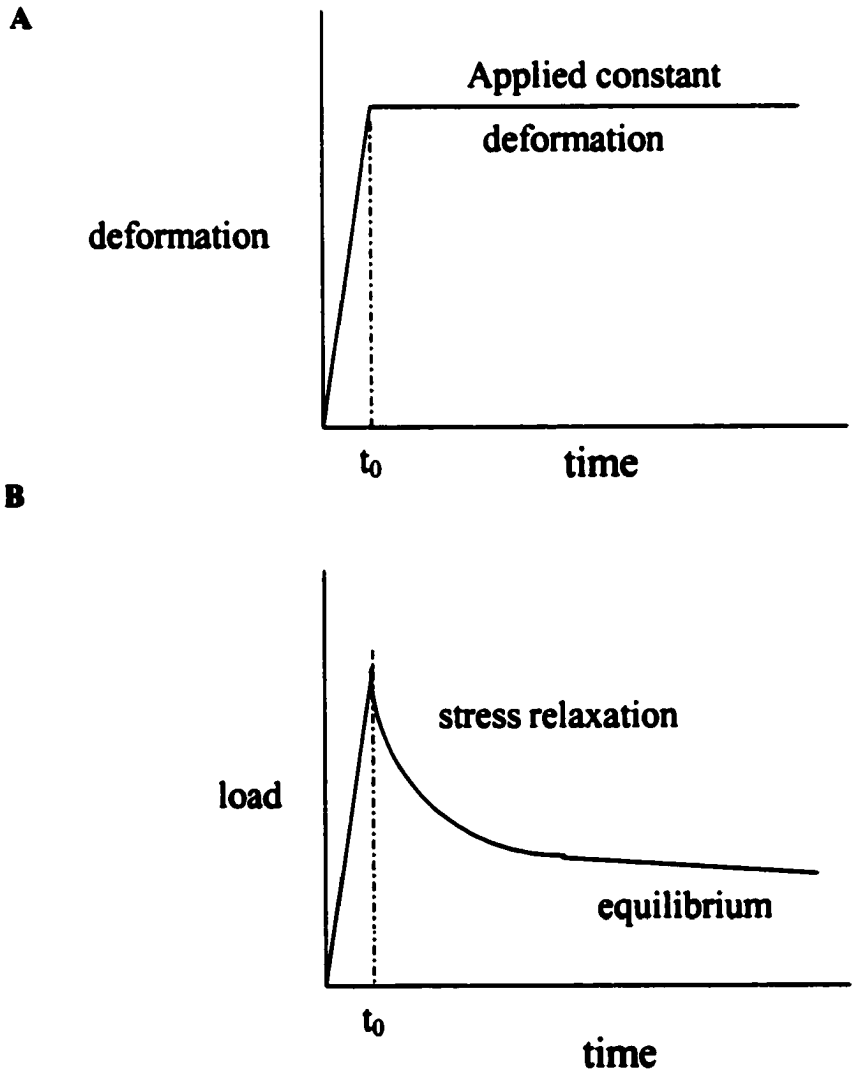

Fig. 6-1: Stress relaxation in a viscoelastic material. (A) Displacement function (B) Stress rise during ramp displacement compression (t<to) followed by stress relaxation (t>to) under constant compression.

Materials and Methods

Normal mature bovine occipital cartilage and normal mature human knee cartilage explants were obtained and punched into 5mm diameter plugs. The plugs were then stored overnight in phosphate buffered saline (PBS) at 4 ^{0}C. Before sampling, the cartilage thickness was measured and the % strain calculated at a tip displacement of δ = 50 μm was 5% and 2% for the bovine and human articular cartilage respectively. After initial contact with the crystal was established via the load cell, IR and tissue relaxation data was then acquired simultaneously to a 50 μm displacement depth.

IR data acquisition: The IFOP was connected to a Bruker spectrometer and a Remspec MCT detector. IR data was acquired using data acquisition software OPUS NT v. 3.

Sampling time: 30 seconds/spectra (~ 85 scans: 4000-900 cm^{-1})

Sampling rate: continuous for 5 minutes (10 IR spectra)

Stress Relaxation data: Stress relaxation data was acquired using a 5-lb load cell connected to a load cell meter and an RS-232 communication system with data acquisition software WINWEDGE v 1.2.

Results

IFOP tip displacement to 50 μm revealed characteristic stress relaxation behavior in both the bovine and human articular cartilage plugs (Fig. 6-2). Time dependent changes in the amide II and III intensities were also noted. Absorbance areas and heights for the amide II and III bands increased linearly for the first 75 seconds, after which there were no significant change in the IR spectra for the bovine and human cartilage samples (Fig. 6-3).

Stress relaxation curve for the mature bovine articular cartilage. (% strain = 5%)

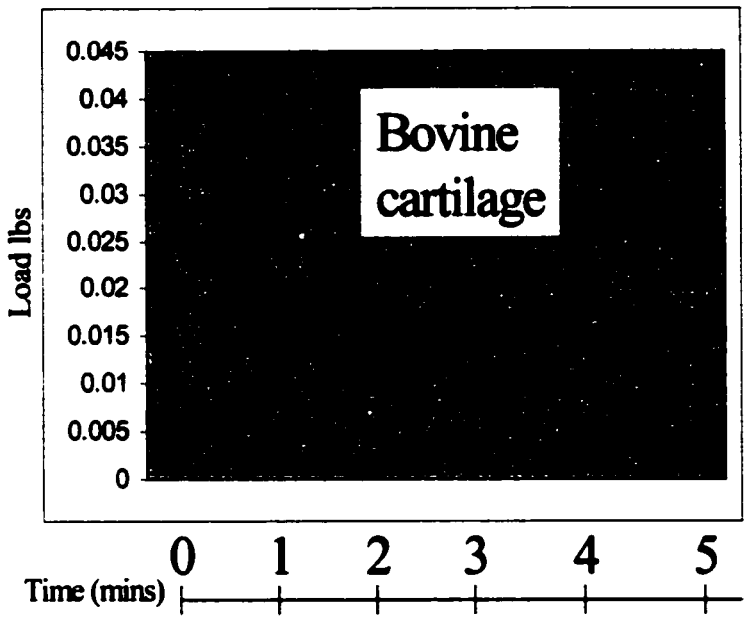

Stress relaxation curve for the mature human articular cartilage. (% strain = 2%)

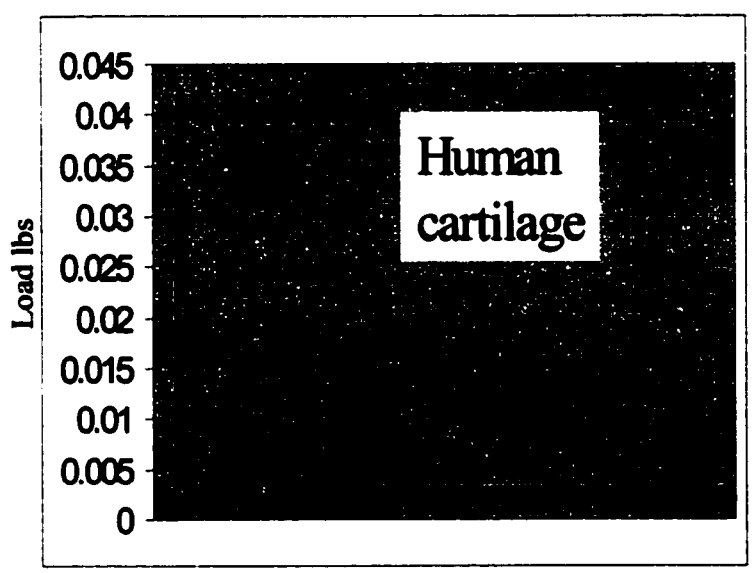

Fig. 6-2: Stress relaxation behavior in both the bovine and human articular cartilage plugs.

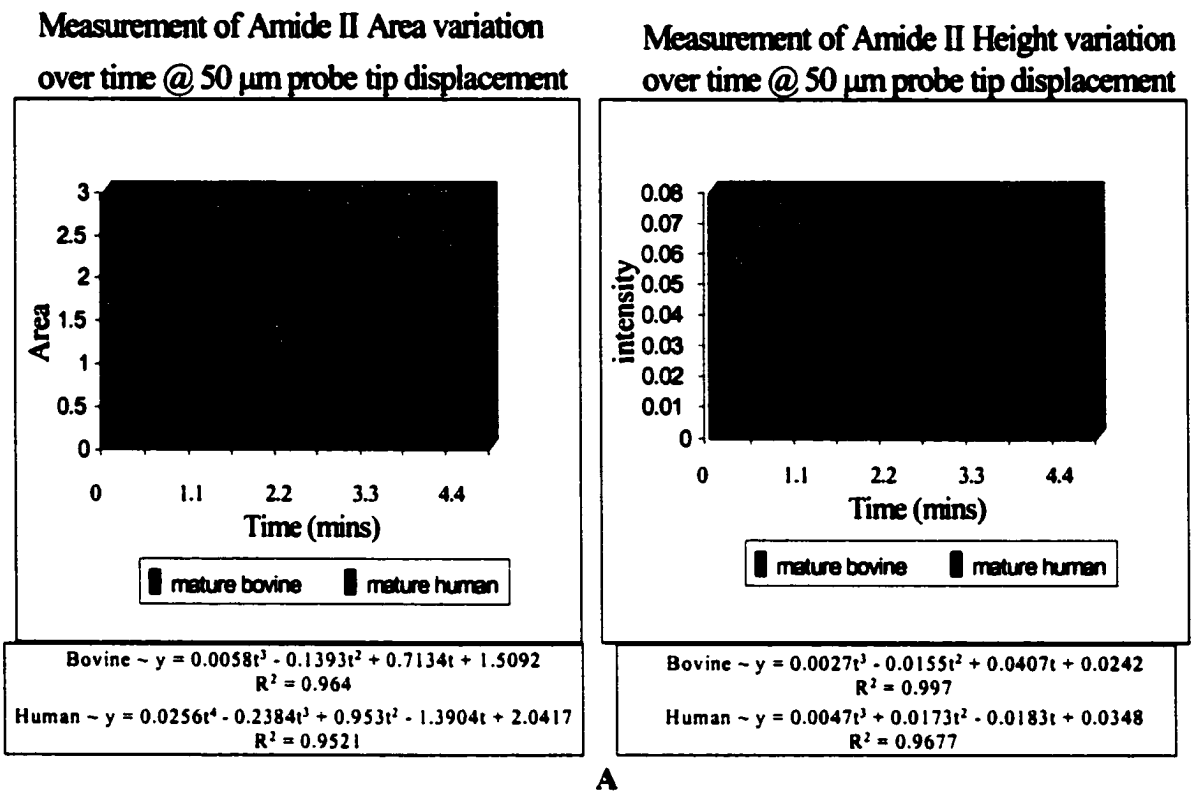

A

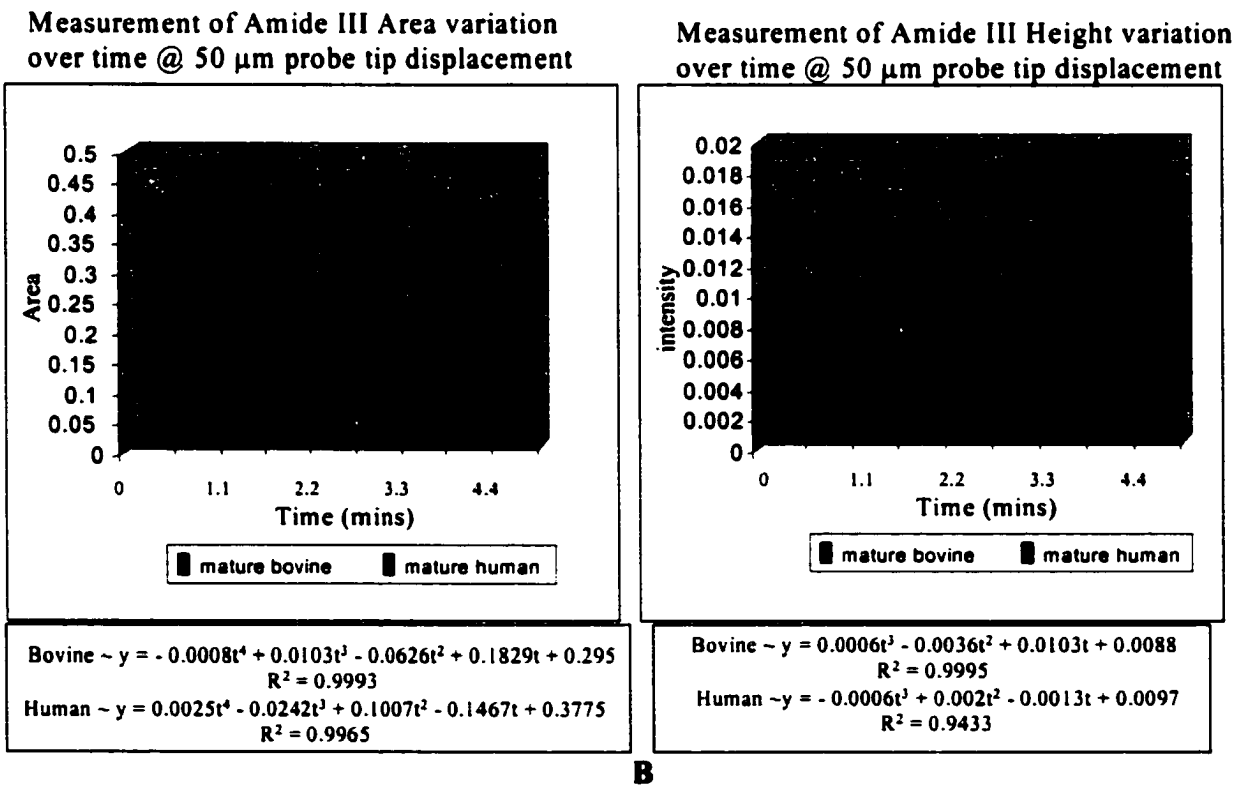

B

Fig.6-3: (A) Amide II and (B) Amide III absorbance vs. time for bovine and human cartilage.

Discussion

The objective of this study was to investigate the effect of stress relaxation within the tissue on the reliability and reproducibility of the IR spectra obtained from the IFOP at a prescribed minimum sampling depth of 50 μm. An understanding of the dynamics involved in our sampling methodology is an important step that fully needs to be understood if the IFOP is to be developed as a diagnostic tool for osteoarthritis.

Our results indicate that the movement of free (unbound) water within the pores of the extracellular matrix lead to a time-dependent response in the IR spectra obtained from the surface of the articular cartilage. More specifically, our study shows that the spectral time-dependent response at a tip displacement of 50 μm is limited to the first 75 seconds of the stress relaxation process. This means that after ~ 75 seconds the surface contact and optical contact created with the crystal is optimized. This also means that further density changes (matrix compaction) associated with the movement of free water away from the sample site are no longer detectable by our method of ATR spectroscopy. Therefore, if our IFOP were to be used clinically for cartilage evaluation, a 50 μm tip displacement would require a delay of ~ 1 minute before data is acquired. This time delay would ensure that the data acquired is accurate and reproducible since sample times are ≥ 1 minute. Obviously greater tip displacements (say 100 μm) may lead to smaller delay times due to higher levels of pressurization with the tissue and faster optimization of the surface contact with the crystal. This potentially may lead to more articular surface damage.

No spectral changes related to the effect of compression on trapped water within the collagen fibrils were observed in any sample during the experiment.

CHAPTER VII

STRUCTURAL ANALYSIS OF DEGENERATIVE CARTILAGE USING AN INFRARED FIBER OPTIC PROBE

Introduction

Osteoarthritis (OA) is a progressively disabling joint disease characterized by degeneration of the articular cartilage resulting in loss of the tissues biomechanical function. It is characterized by the progressive loss of the articular cartilage, followed by sclerosis of the subchondral bone and the formation of subchondral bone cysts and osteophytes. Such degenerative disorders of the articular cartilage are usually diagnosed only after cartilage loss and surface irregularities (fibrillations, clefts or fissures) are observed on radiographic imaging. At this point, end-stage degenerative joint disease is usually quite advanced and total joint replacement procedures may ultimately be necessary to restore pain-free mobility to the joint. Currently, there are no available means of diagnosing the disease process at an early stage.

Prior studies have shown that osteoarthritis (OA) appears to start at the cellular level due to trauma or improper loading on its structure. This disrupts homeostasis and leads to pathognomonic changes within the tissue that become more severe as the disease progresses. Consequently, articular cartilage composition, molecular and ultrastructral organizations, and biomechanical properties are altered as catabolic activity within the extracellular matrix begins to dominate. This results in a denatured collagen network and the loss of proteoglycans from the tissues extracellular matrix.

In this study, the infrared fiber optic probe (IFOP) was used to evaluate degenerative damage in human articular cartilage. Information on quantity and structure of articular surface proteins, primarily type II collagen will be obtained from each

sample. It is our hypothesis that the ability of the IFOP to distinguish between normal and degraded articular cartilage based on spectral changes will be demonstrated.

Materials and Methods

Twelve arthritic human tibial plateaus (TP) were obtained during knee replacement surgery, and analyzed using the IFOP under an IRB-approved protocol. Each specimen was secured on the micrometer driven load cell apparatus and the fiber optic flat-tipped ZnS ATR crystal with a 1-mm area of surface contact was placed in contact with sites visually identified and graded as either grossly normal (no obvious macroscopic damage) or degraded (fibrillations, clefts or fissures present), corresponding to Collins Scale (13,33) grade 1 and grade 3 respectively (figure. Fig.7-1).

For each site, 256 scans were acquired, averaged and referenced to a saline background using Grams/32 software. For all spectra, a Savitsky Golay 17 point smooth was applied (Fig. 7-2). The spectra were baselined and the type II collagen absorbances were monitored in the 1590-1480 cm^{-1}, 1338 cm^{-1} and 1300-1200 cm^{-1} infrared regions. (Table 1). Spectra were evaluated for changes in area and peak intensity in these regions. Area changes were observed in the amide II and peak 1338 cm^{-1} absorbance, while contour changes (peak intensity) were observed in the amide III absorbance region. Area and peak intensity ratios were then calculated. Using ratios avoids errors that would otherwise be incurred by using pure absorbances (concentration dependent) that change with tip depth. The following parameters were calculated based on absorbance area and peak intensities at specific frequencies: amide II/peak 1338 area ratio and 1238/1227 cm^{-1} peak ratio. Based on our findings in chapter II it was assumed that negligible signal from proteoglycan was present in the spectra.

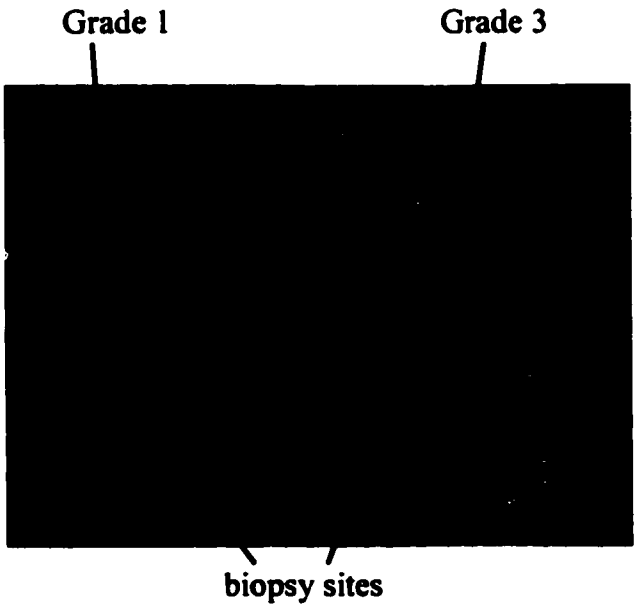

Fig. 7-1: Collins scale grade 1 & 3 sites on a human tibial plateau.

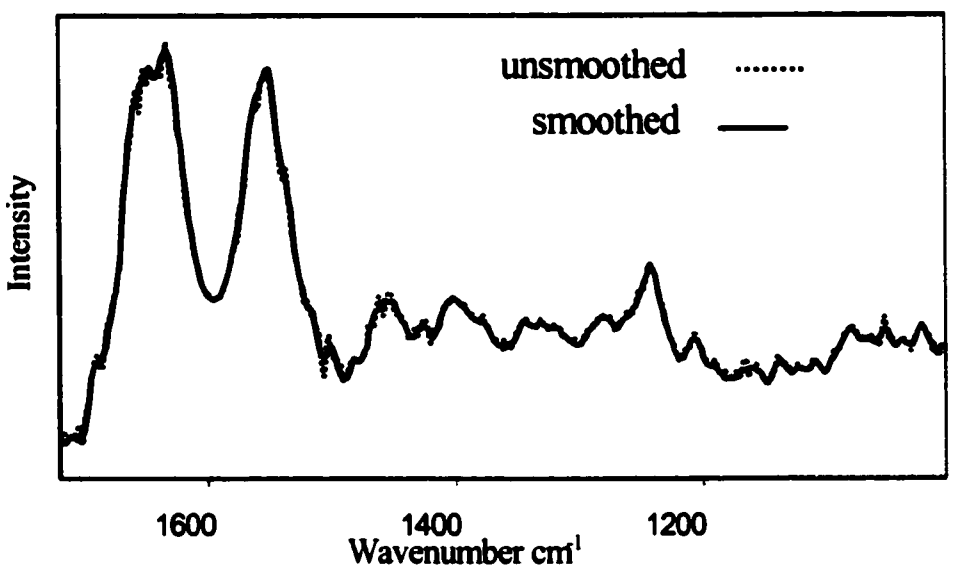

Fig. 7-2: 17 point Savitsky-Golay smoothed and unsmoothed IFOP spectra.

Table 7-I: Analyzed Type II Collagen Infrared Frequencies

Bond Vibrations	Wavenumber
Amide II C-N stretch, N-H bend combination	1590-1480 cm^{-1}
Amide III C-N stretch, N-H bend	1300-1200 cm^{-1}
Peak 1338 side chain vibrations	1338 cm^{-1}

FTIR Imaging (FT-IRI): For comparison FT-IRI analysis was performed on selected tissues previously analyzed by the IFOP. Our gold standard FT-IR Imaging system is a reliable and well-established method currently used in scientific research. This method serves as a valid reference due to the high quality of the acquired spectra (obtained in transmission mode as opposed to reflection). For analysis graded 5mm biopsy plugs (Fig. 7-1) were flash frozen and cryo-sectioned directly onto barium fluoride windows in 6 μm sections for eight of the twelve arthritic human tibial plateaus. The BioRad (Cambridge, MA) UMA 300A FTIR microscope with an FTS-60A step-scanning FTIR spectrometer and a 64x64 MCT FPA detector (Stingray Imaging Spectrometer) was used to acquire spectra at 8 cm^{-1} resolution under N_2 purge. Information on collagen content and distribution was obtained from a 400 x 400 μm^2 region, resulting in 4,096 individual spectra for each sample. Using the amide I absorbance band as an image peak, collagen distribution within the superficial (surface) zone was identified for each sample (Fig. 7-3). Twenty individual surface spectra were randomly chosen from the superficial zone of each sample for comparison with the IFOP data.

Statistical Analysis: For each parameter examined (amide II/peak 1338 area ratio and 1238/1227 cm^{-1} peak ratio), mean values and standard deviations were obtained. A paired T-test was utilized to determine significant differences at $p < 0.05$.

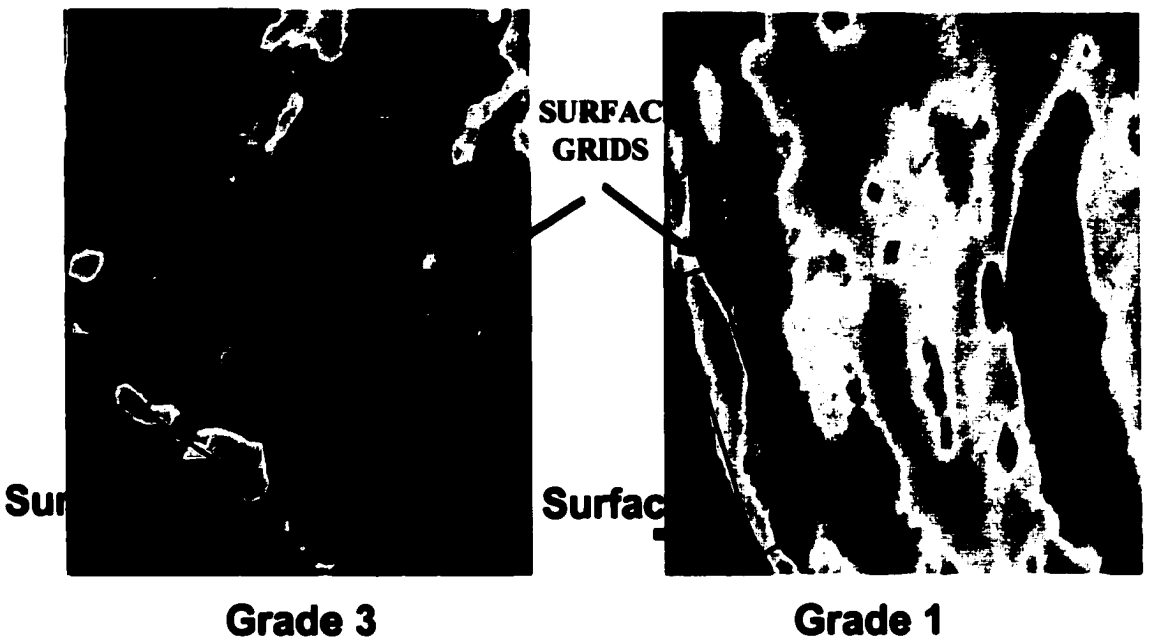

Fig. 7-3: Superficial zone area in a grade 1 & 3 cartilage sample.

Results

It has previously been established that the spectra obtained from the superficial zone of articular cartilage by FT-IRI arise primarily from Type II collagen (34). Spectral analysis on the twelve arthritic human tibial plateaus revealed consistent changes between grade 1 and grade 3 sites. Specifically, an increased Amide II/peak 1338 area ratio ($p=0.034$) and a decreased 1238/1227 cm^{-1} peak ratio ($p=0.017$) are observed for the more degraded tissues (Fig. 7-4).

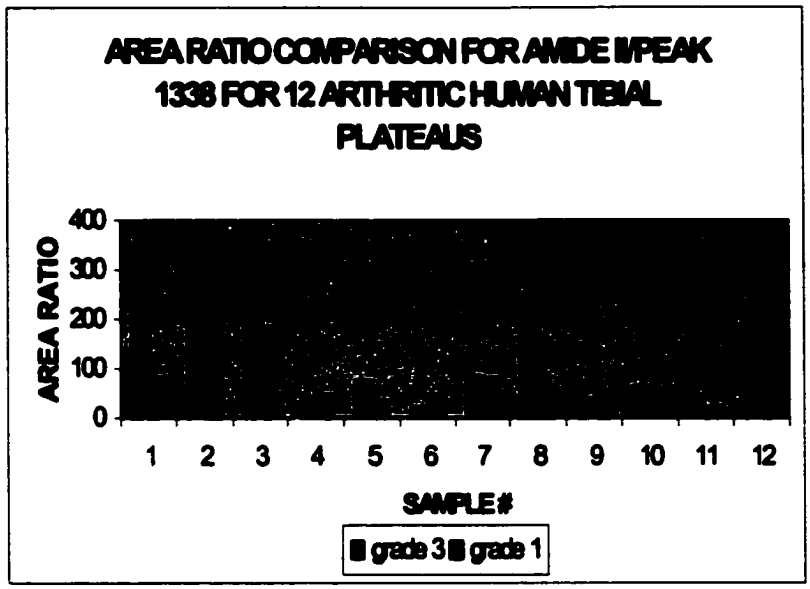

Amide II/1338 Area Ratio

	1	2	3	4	5	6	7	8	9	10	11	12
grade 3	255	386.8	382.8	28.4	75.68	20.1	85.4	250.6	39	63.5	18	61.5
grade 1	80	243.7	184.5	44.6	35.3	44.4	78	63	20.4	57.4	22	59

A

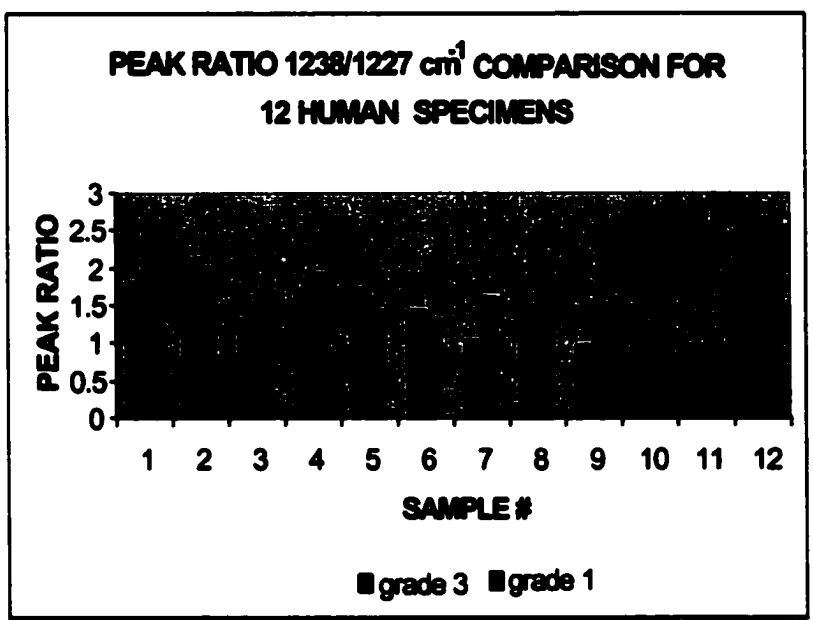

1238/1227 cm^{-1} Peak Ratio

	1	2	3	4	5	6	7	8	9	10	11	12
grade 3	1.8	2.1	1.3	1.7	1.7	1.4	1	1.45	0.98	1.2	0.95	1.9
grade 1	2.4	2	1.7	1.9	1.4	1.3	1.6	2.2	1.5	1.25	1.12	2.3

B

Fig. 7-4: IFOP - (A) amide II/peak 1338 area ratio and (B)1238/1227 cm^{-1} peak ratio comparison.

FTIR Imaging (FT-IRI): FTIR Imaging analysis (gold standard) also revealed similar changes between grade 1 and grade 3 sites for the two previously mentioned parameters. For eight of the twelve arthritic human tibial plateaus analyzed using FTIR Imaging, amide II/peak 1338 area ratio increased ($p < 0.001$) and 1238/1227 cm^{-1} peak ratio ($p < 0.001$) decreased between grade 1 and grade 3 sites. All the changes observed with FTIR Imaging analysis were referenced to normal cartilage (Collins scale-grade 0) (Fig. 7-5). Grade 0 cartilage shows no degenerative morphological changes.

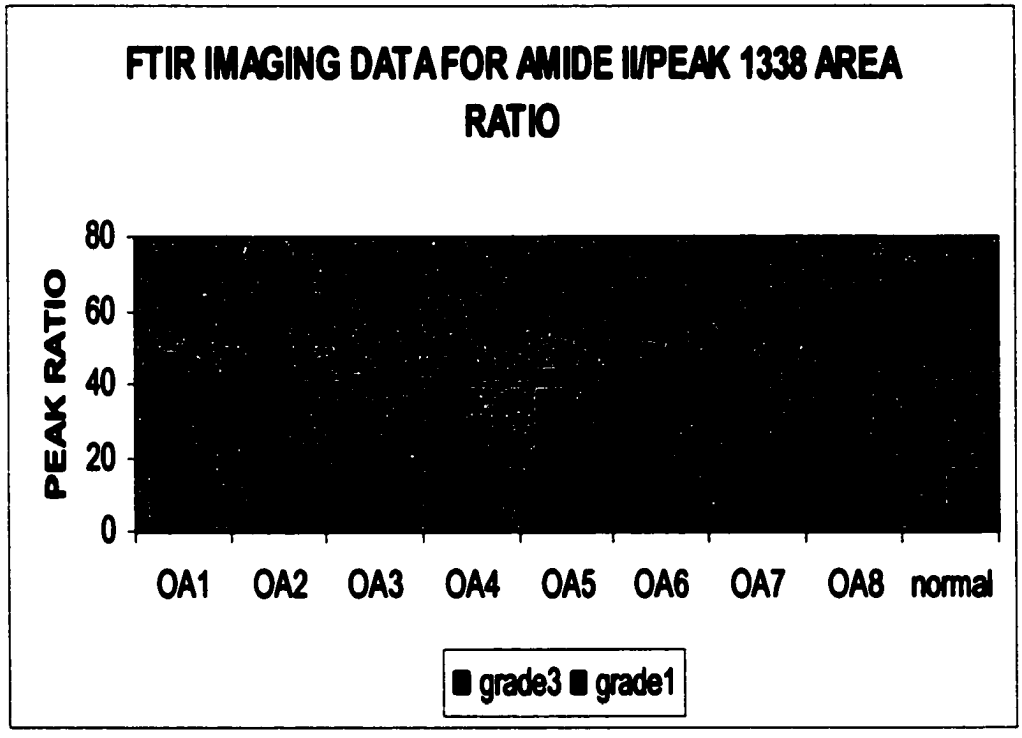

	Amide II/1338 Area Ratio (mean values-n=20 for each patient)								
	OA1	OA2	OA3	OA4	OA5	OA6	OA7	OA8	normal
grade3	38.20	59.19	34.60	29.81	37.42	34.24	40.18	63.64	mean
grade1	20.88	22.68	22.00	16.97	19.11	17.87	21.71	23.68	15.44
STD(g3)	9.50	16.38	6.80	7.01	6.00	15.86	12.48	4.28	STD
STD(g1)	1.88	1.34	3.00	5.25	1.99	0.63	1.20	1.47	2.75

A

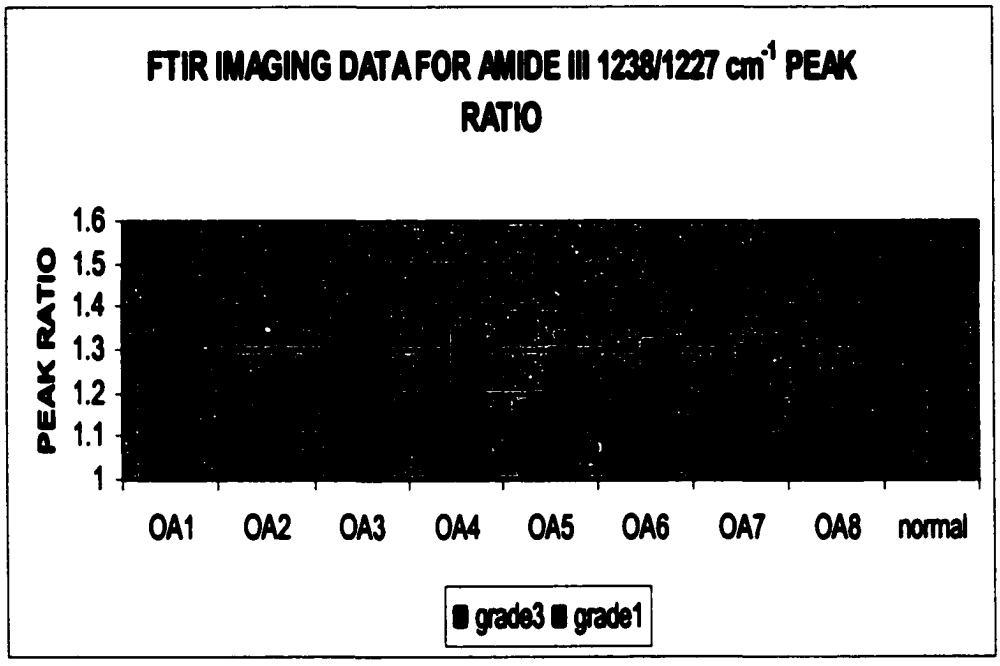

1238/1227 cm^{-1} Peak Ratio (mean values-n=20 for each patient)

	OA1	OA2	OA3	OA4	OA5	OA6	OA7	OA8	normal
grade3	1.30078	1.136863	1.4	1.215809	1.179471	1.207247	1.183957	1.132954	mean
grade1	1.46434	1.263412	1.5	1.346916	1.298855	1.320858	1.305222	1.257528	1.5
STD(g3)	0.03335	0.028063	0.02153	0.025286	0.015943	0.03845	0.02453	0.012966	STD
STD(g1)	0.07718	0.038012	0.0463	0.045229	0.03422	0.056156	0.02529	0.031877	0.06

B

Fig. 7-5: FTIR Imaging - (A) amide II/peak 1338 area ratio and (B) 1238/1227 cm^{-1} peak ratio comparison.

Discussion

In this study we investigated the potential use of an Infrared Fiber Optic Probe (IFOP) as a tool in detecting molecular changes in type II collagen in 12 arthritic human tibial plateaus. Our analysis revealed that the IFOP shows good promise as a possible diagnostic tool for detecting changes involved in the degradation of articular cartilage. Although this analysis was based on the comparison with cartilage (grade 3) that was obviously arthritic, it is our hope that with better developed multi-variate data processing

methods we will be able to monitor the more subtle changes related to early cartilage degeneration. For the 12 plateaus analyzed, compared grade 1 and grade 3 sites showed consistent changes between both Amide II/peak 1338 area ratio and 1238/1227 cm^{-1} peak ratio. More specifically, from grade 1 to grade 3, an increased Amide II/peak 1338 area ratio and a decreased 1238/1227 cm^{-1} peak ratio are observed. These IFOP findings were further corroborated by FTIR imaging analysis.

In progressive articular cartilage degeneration, specific matrix metalloproteinases (MMPs) are upregulated by the chondrocyte cells thereby initiating the denaturation of the type II collagen fibrils. This enzymatic activity (primarily due to the MMPs 1,8&13) - collagenases) result in the cleavage of the collagen triple helix structure at a single site, thus producing approximately ¼ and ¾ length denatured alpha (α) chain fragments (35). Over time these molecular changes gradually lead to further denaturation and failure of the extracellular fibrillar network due to the unraveling of the collagen molecule. These destructive biochemical changes that occur within diseased cartilage translate into observable IR parameters. The 1338 cm^{-1} collagen band (CH_2 side chain vibrations) is sensitive to the order of the triple helix and decreases in intensity as the collagen denatures (22,36). This leads to an increased amide II/peak 1338 area ratio in diseased states. Also, a change in the very complex amide III absorption leads to a decrease in the 1238/1227 cm^{-1} peak ratio with collagen degradation (22).

These molecular changes in the collagen network form the basis for the FTIR study. The reliability of the IFOP in detecting collagen in the superficial zone of cartilage is well established, and has been verified by FTIR imaging spectroscopy. In comparing normal and arthritic cartilage, changes were observed in the collagen spectra. It is thus

the conclusion that the IR changes observed here are associated with the unraveling of the collagen triple helix structure due to the activity of collagenase. This data suggests that the IFOP is sensitive to changes in articular cartilage that likely arise from molecular changes within the collagen extracellular network.

Chapter VIII

FTIR Imaging of Collagenase Treated Bovine Cartilage

Introduction

The use of FTIR spectroscopy to investigate normal vs. arthritic human articular cartilage (as shown in the previous chapter) revealed consistent changes in specific IR parameters. It is our hypothesis that these changes are attributed to the direct action of collagenase on the collagen fiber network within the superficial zone. These densely packed collagen fibrils which are aligned parallel to the articular surface (polarization sensitive), provide tensile strength and monitor the movement of solutes in and out of the cartilage. The effect of collagenase on these collagen fibrils is to cause cleavage of the triple helical structure of peripheral molecules at a single site ¾ distance from the N-terminal end. This leads to ¾ and ¼ length fragments that can be detected by specific antibodies Col2- ¾C_{short} and Col2-¼N1 that react only to cleaved carboxy (COOH-) terminal and amino (NH_2.) terminal neoepitopes respectively (35). This type of breakdown of the collagen architecture as seen with the progression of OA also results in the loss of polarization sensitivity that is specific to the orientation of collagen parallel to the articular surface.

In this study, the treatment of collagenase (MMP-1) on the articular surface of normal bovine cartilage explants is investigated using FTIR Imaging spectroscopy (our gold standard). Our intention is to show that the catabolic action of collagenase on the collagen fibrils at the articular surface can result in similar changes to the IR parameters previously observed between normal and arthritic human cartilage using the IFOP.

Polarization data will also be collected to obtain information on the disorientation of the collagen fibers with collagenase treatment.

Materials and Methods

Twelve full-depth cartilage explant plugs were obtained from an adult bovine knee joint immediately after death. Each 7-mm diameter plug (~ 2 mm thick) was punched and removed from the subchondral bone with the aid of a scalpel. Collagenase treatment was applied to the articular surface in the Laboratory for Soft Tissue Research at The Hospital for Special Surgery (Dr. Chris Chen). Six collagenase treated plugs (3-15minutes and 3-30minutes) and six un-treated (control) explant plugs were produced. For the treated explants, collagenase activity was promoted in one direction (z) only (superficial zone → deep zone) by placing the plugs in a cylindrical chamber in which the sides were confined. After placing in OCT embedding media (Miles Inc., Elkhart, IN), the plugs were flash frozen in liquid nitrogen and stored at -70^{0} C. Six 6-μm slices were cryosectioned from each explant plug. Three were placed on BaF2 windows for FTIR Imaging analysis, while the remaining three were placed on histology slides for immunohistochemical staining for collagenase-generated neoepitopes. Immunohistochemistry using antibidies Col2-¾C_{short} and Col2-¼N1 was performed by Peggy Lin at the Laboratory for Soft Tissue Research at The Hospital for Special Surgery

The BioRad (Cambridge, MA) UMA 300A FTIR microscope with an FTS-60A step-scanning FTIR spectrometer and a 64x64 MCT FPA detector (Stingray Imaging Spectrometer) was used to acquire spectra for each sample at a 8 cm^{-1} resolution under N_2 purge. Data were collected from a 400 x 400-μm^2 region mapped to the individual elements of the array detector, resulting in 4,096 individual spectra. Polarization data were acquired by placement of a wire grid polarizer between the sample and the incident

IR radiation. Spectra were acquired with the IR radiation polarized parallel and perpendicular to the articular surface.

Imaging data were analyzed with WinIR Pro software v.2.5 (BioRad). Spectra (25 per section) used for IR parameter analysis were obtained from the superficial zone where the densely packed collagen fibrils are aligned parallel to the articular surface. For each sample, areas under the amide II (1550 cm^{-1}) and collagen 1338 cm^{-1} peak were calculated along with amide III peak intensities at 1238 and 1227 wavenumbers. Integrated area ratios (amide II/ peak 1338) and peak intensity ratios (1238 cm^{-1}/1227 cm^{-1}) were calculated, averaged and compared for the untreated (control), 15 and 30 minute collagenase treated sections. The type II collagen amide I absorbance arises primarily from bond vibrations (carbonyl C=0 stretch) that are perpendicular to those arising from amide II (36). Thus, in the polarized experiments, the ratio of the areas of amide I:amide II absorbance in one polarization (favorable to surface collagen orientation) was calculated and imaged as an indicator of orientation. Therefore, a larger amide I:amide II absorbance ratio represents a higher population of collagen fibrils oriented parallel to the cartilage articular surface. The same grid locations used for IR parameter analysis were also used to analyze the polarization data.

Results

Histological assessment using the Col2- ¼C_{short} antibody resulted in positive staining (collagenase activity) for the collagenase treated sections only (Fig. 8-1). Positive staining was observed through most of the superficial zone for both the 15 minute and 30 minute treated specimens. A comparison of the IR parameters (amide II/ peak 1338 area ratio and 1238 cm^{-1}/1227 cm^{-1} peak ratio) between the treated and un-treated specimens showed good correlation with the results obtained from the IFOP.

With collagenase treatment, the amide II/ peak 1338 area ratio increased while the 1238 cm^{-1}/1227 cm^{-1} peak ratio decreased (Fig.8-2). Using the same articular surface grid locations, analysis of the polarization data (collagen orientation parallel to articular surface) revealed a decrease in the amide I/II area ratio with collagenase treatment (Fig. 8-3,4). This finding is consistent with our hypothesis that the amide I/II area ratio is a measure of collagen fiber orientation. Also for the treated specimens, spectral analysis below the area of collagenase activity revealed no change in the amide I/II area ratio between the treated and un-treated specimens (Fig. 8-5).

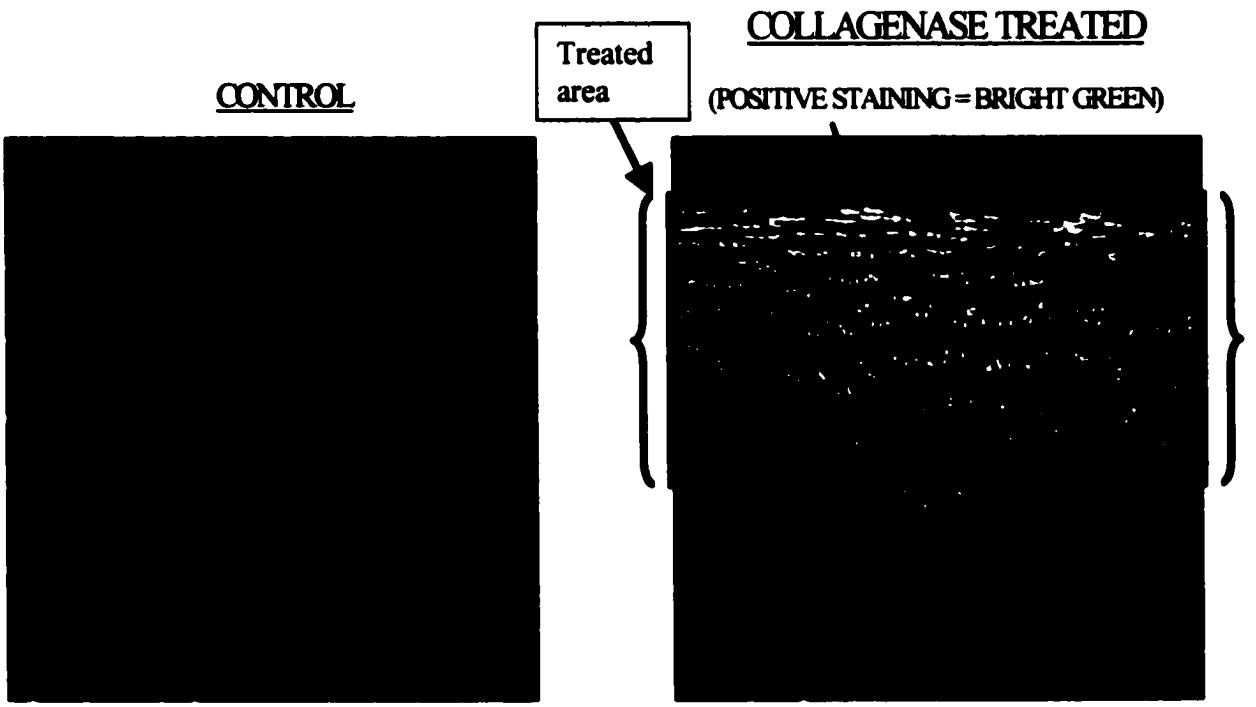

Fig. 8-1: Antibodies show positive stain (bright green) for collagenase activity in treated specimens (boxed area).

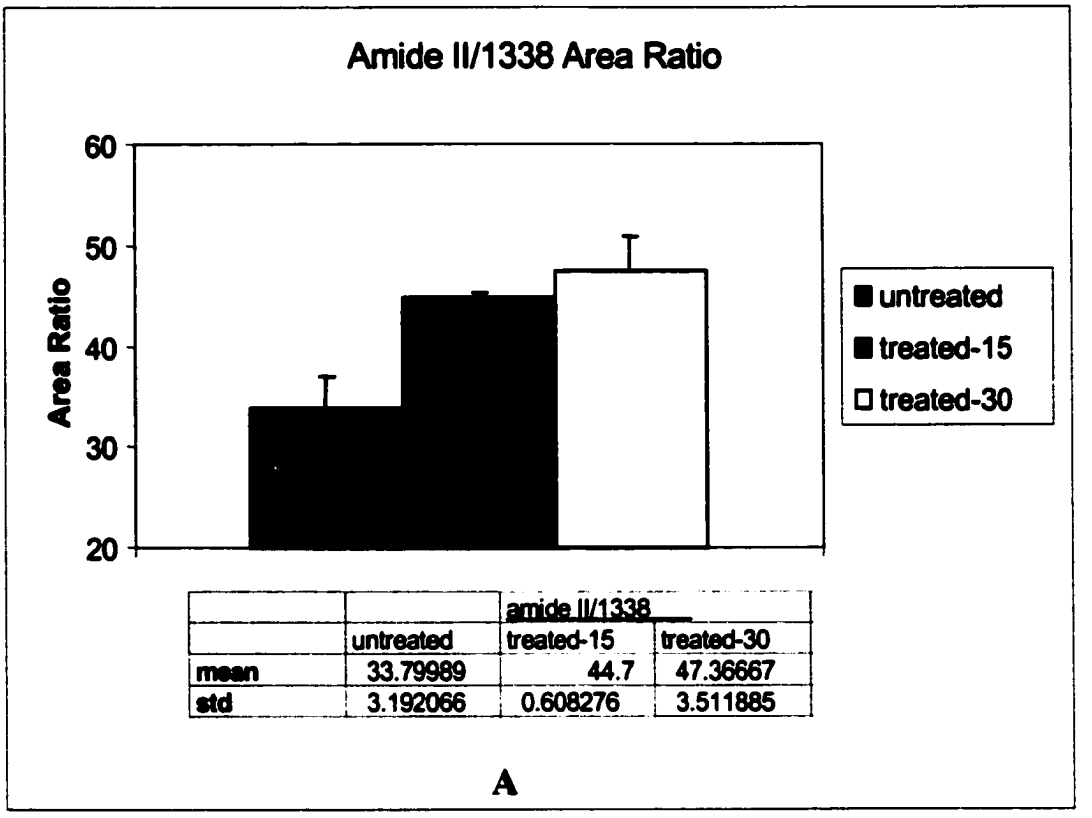

		amide II/1338	
	untreated	treated-15	treated-30
mean	33.79989	44.7	47.36667
std	3.192066	0.608276	3.511885

A

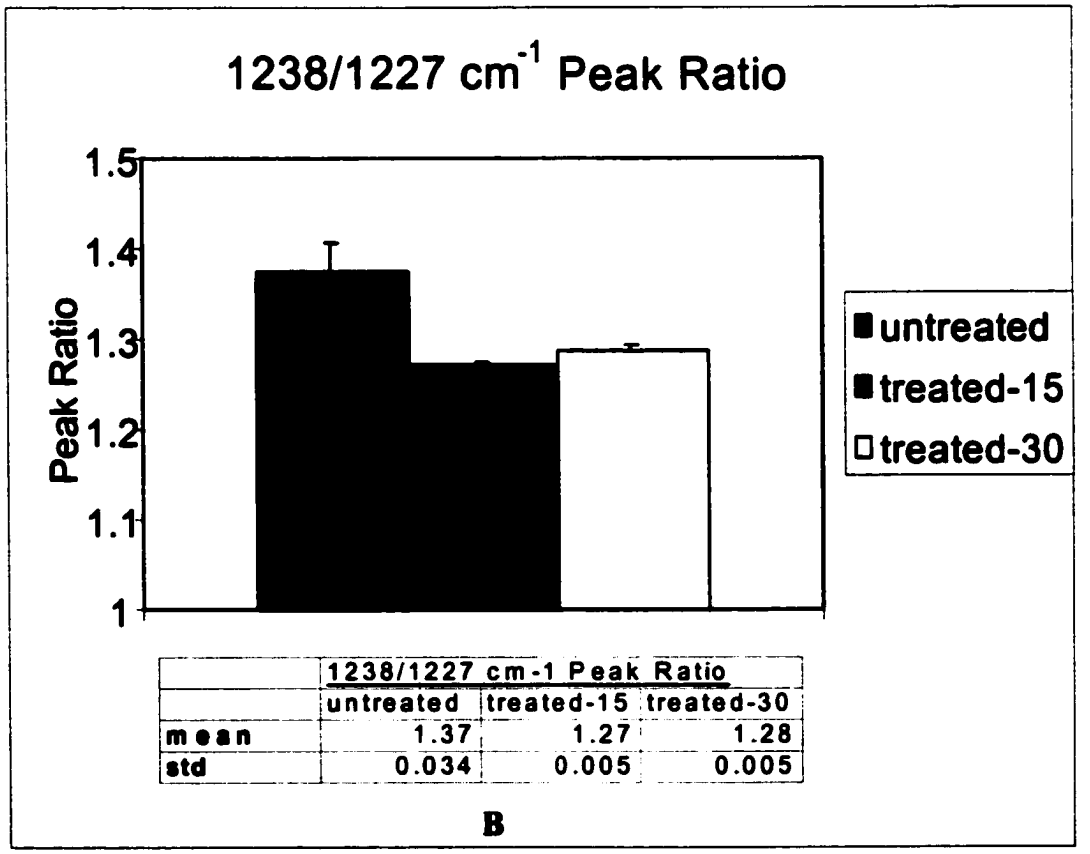

	1238/1227 cm-1 Peak Ratio		
	untreated	treated-15	treated-30
mean	1.37	1.27	1.28
std	0.034	0.005	0.005

B

Fig. 8-2: (A) Amide II/Peak 1338 area ratio change with collagenase treatment.
(B) 1238 cm-1/1227cm-1 peak ratio change with collagenase treatment.

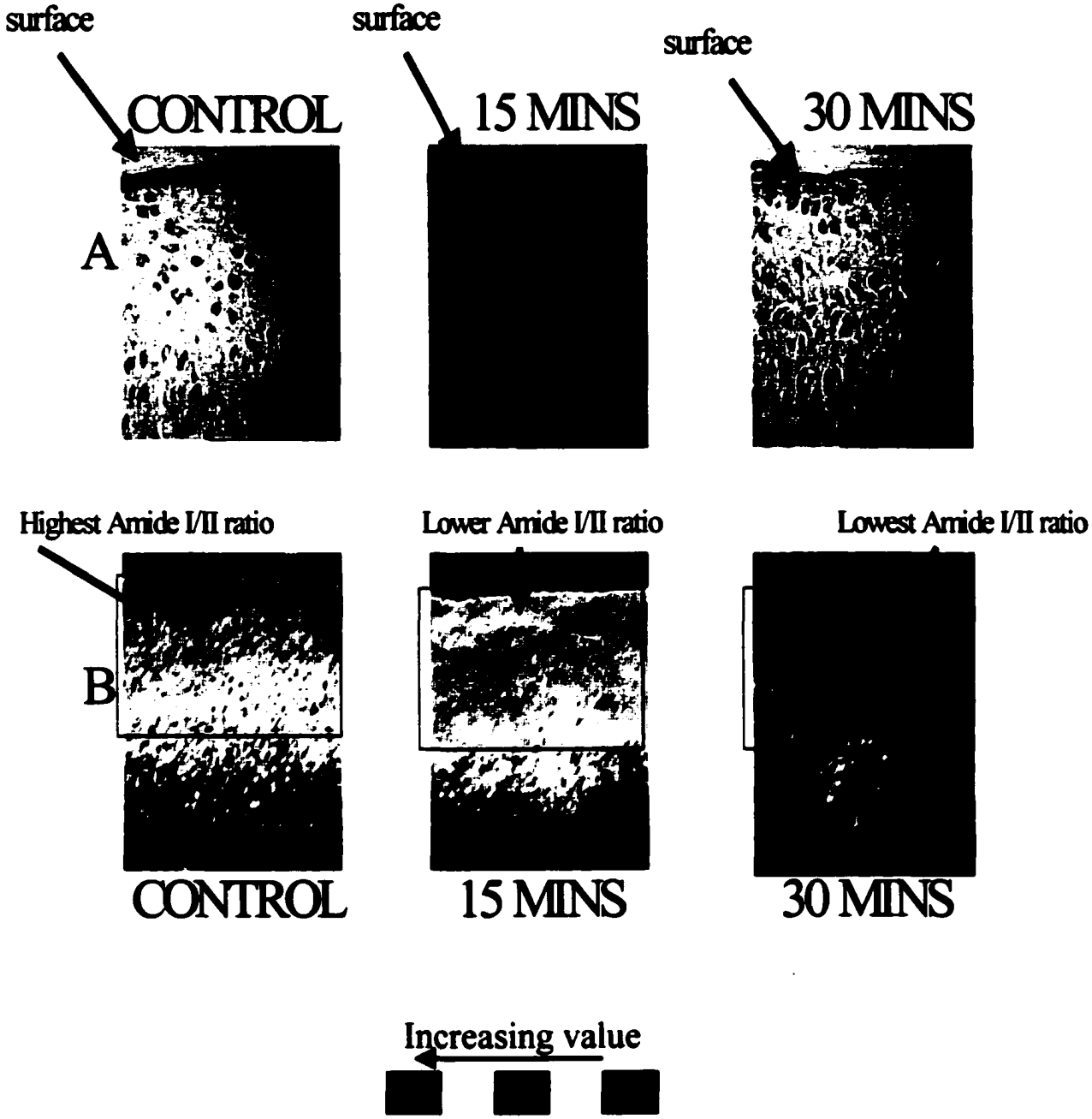

Fig. 8-3: (A) Microscope pictures of the sections on the BaF_2 window before FTIR data acquisition (notice the 30 minute section shows visible evidence of collagenase activity). (B) FTIR imaging change in the superficial zone amide I/II area ratio with collagenase activity (collagen parallel to articular surface).

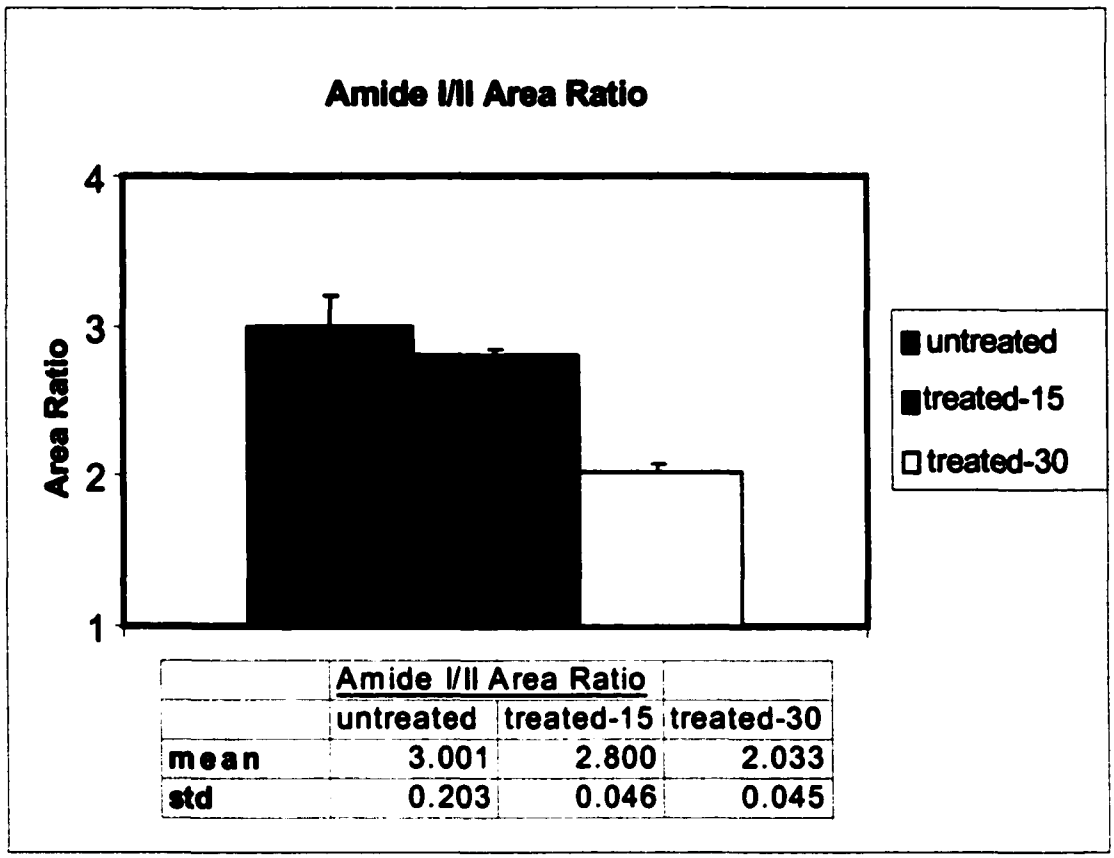

	Amide I/II Area Ratio		
	untreated	treated-15	treated-30
mean	3.001	2.800	2.033
std	0.203	0.046	0.045

Fig. 8-4: Amide I/II area ratio change with collagenase treatment.

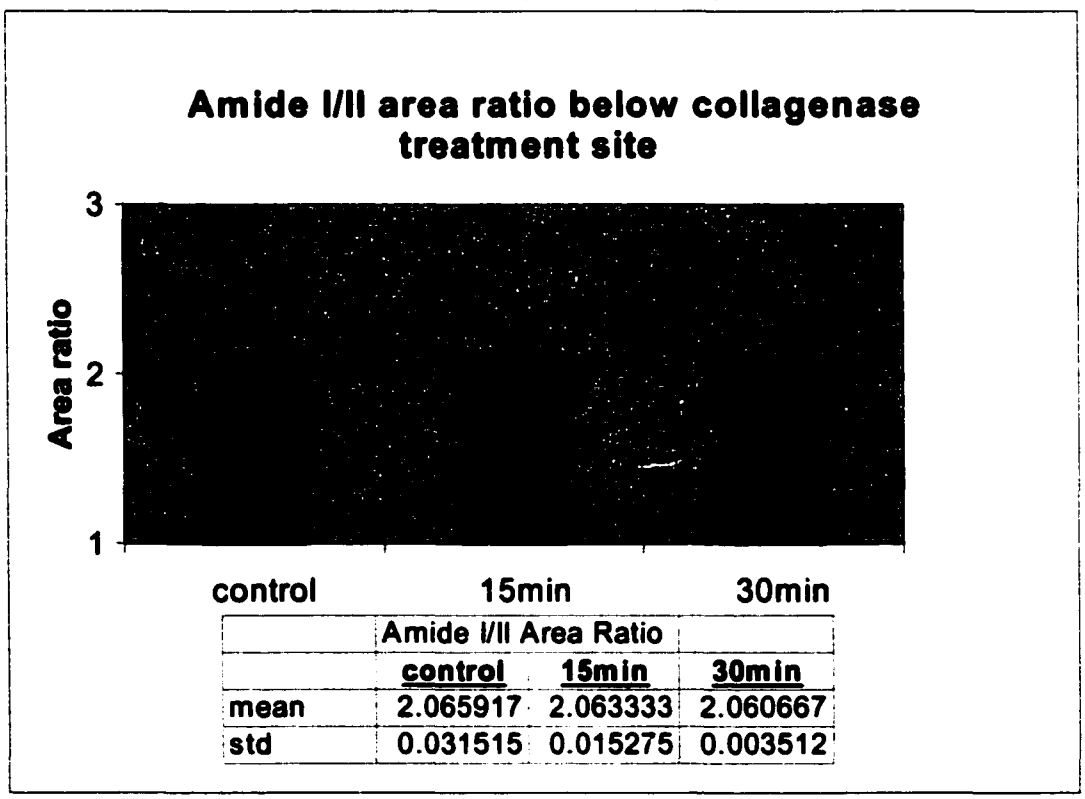

	Amide I/II Area Ratio		
	control	15min	30min
mean	2.065917	2.063333	2.060667
std	0.031515	0.015275	0.003512

Fig. 8-5: Amide I/II area ratio change below the collagenase treatment area.

Discussion

This study demonstrates that the IFOP spectral changes observed in the study of human arthritic articular cartilage are a likely result from the activity of collagenases on the type II collagen fibrillar arrangement and, that these spectral changes are related to the specific molecular disruption that occurs as the collagen molecule is cleaved ¾ length from the N-terminal. More specifically, with cleavage of the molecule we see a dominant decrease in the 1338 cm^{-1} collagen absorbance band, leading to an increase in the amide II/1338 cm^{-1} area ratio. Similarly, there are changes in the amide III absorbance contour that lead to a decrease in the 1238 cm^{-1}/1227 cm^{-1} peak ratio with collagen cleavage (22,36). To match our findings with collagenase activity, all the specimens prepared in this experiment were stained for collagenase generated neoepitopes using the Col2- ¾C_{short} and Col2-¼N1 antibodies. All the treated sections showed positive staining for collagenase activity through most of the superficial zone. FTIR images generated from the polarized amide I/II area ratios enabled visualization of the disorientation that occurs with denaturing collagen. For treated specimens, analysis of this data showed an inverse proportionality between collagen organization (orientation) and collagenase treatment times (Fig.8-4). Control specimens naturally had the highest amide I/II area ratios (negative staining for collagenase activity). This finding clearly presents us with a new technique capable of detecting collagen changes. As an internal control, spectral analysis below the area of collagenase activity (~ 350 μm below articular surface) revealed no change in the amide I/II area ratio between the treated and un-treated specimens (Fig 8-5). This was inline with what was expected.

The fact that we can use IR spectroscopy to detect surface collagen architecture and molecular changes proves very promising, since these changes precede macroscopic

surface changes such as ruptures and fibrillations that occur with the progression of OA. The use of our FTIR Imaging gold standard clearly illuminates the potential of the IFOP as a reliable tool for the diagnosis and treatment of osteoarthritis.

CHAPTER IX

Detection of Degenerative Cartilage in a Rabbit Model of OA by Infrared Fiber Optic Probe

Introduction

The ultimate goal in developing the IFOP is for it to be used as an arthroscopic tool (during joint surgery) for evaluation of cartilage integrity. Such evaluation may involve determination of the overall integrity of the articular surface or more specifically determination on the integration of tissue-engineered cartilage (used to fill surface defects) with existing cartilage.

In this study, we investigate IFOP spectral parameters associated with articular cartilage degradation in a rabbit model of OA.

Materials and Methods

Under an IACUC-approved protocol, surgery was performed on the right knee of 6 month old female New Zealand white rabbits to create osteoarthritic changes similar to that described in the Hulth-Tehlag Model (37). The surgery involved transection of the anterior cruciate ligament and the posterior cruciate ligament and excision of the medial meniscus. The left knee was sham-operated. At 2, 3, 4, 6, and 9 weeks post-surgery, animals were evaluated by arthroscopy and infrared fiber optic probe. The distal femoral condyle of the rabbits was examined by IFOP by gently placing the probe in contact with the surface of the cartilage. Spectral data was obtained and comparisons in peak heights and areas made between operative (degraded-right) and sham-operated (control-left) sites. The areas and intensities of the type II collagen absorbances (amide II, III & peak

1338) were monitored in the 1590-1480 cm^{-1} and 1300-1200 cm^{-1} infrared regions respectively.

Results

In this rabbit model, by 4 weeks-post surgery there were degradative changes in the cartilage evidenced as clefting in the superficial layers. The superficial layers were almost totally deteriorated by 9 weeks post-surgery. There was no obvious change with time in the control cartilage. Consistent spectral changes were found between cartilage from the control and operative (right) joints (Figs. 8-1,2). Detectable changes were found in the amide III region, where the intensity ratios of the 1238 cm^{-1}/1227 cm^{-1} peak decreased ($p = 0.03$, paired t-test) with degradation. Also, the ratio of the amide II area to the 1338 cm^{-1} area absorbance tended to increase ($p = 0.13$, paired t-test) with degradation.

Fig. 9-1: 1238 cm^{-1}/1227 cm^{-1} area ratio in rabbit OA model.

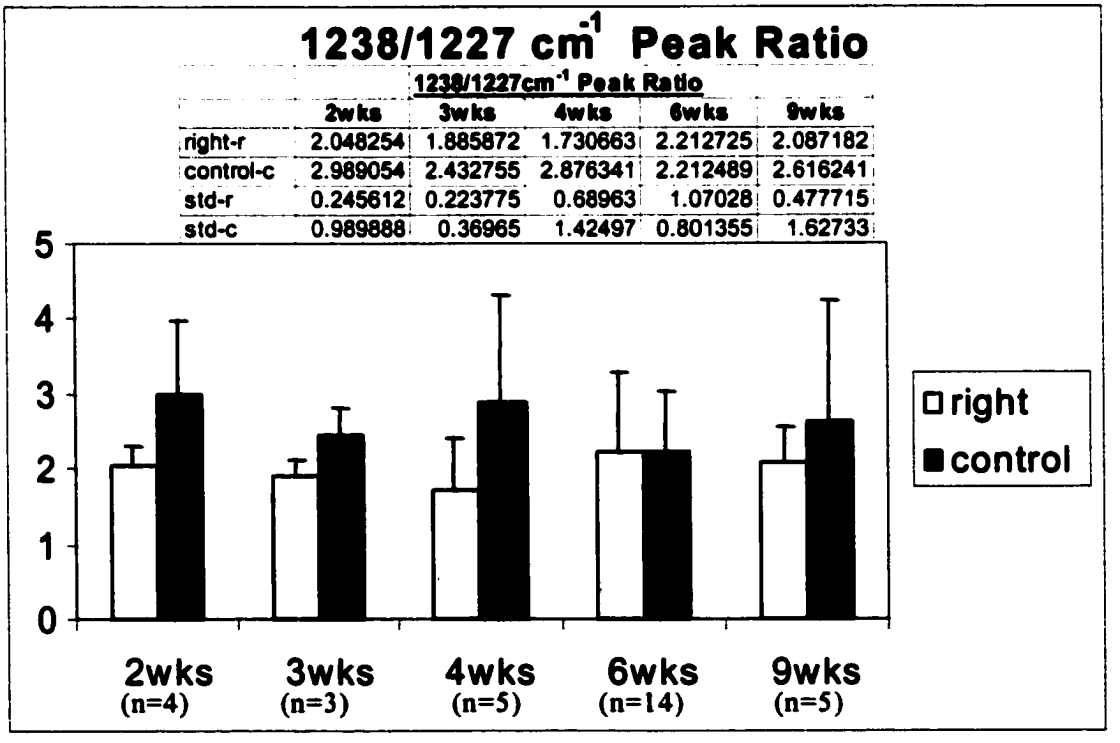

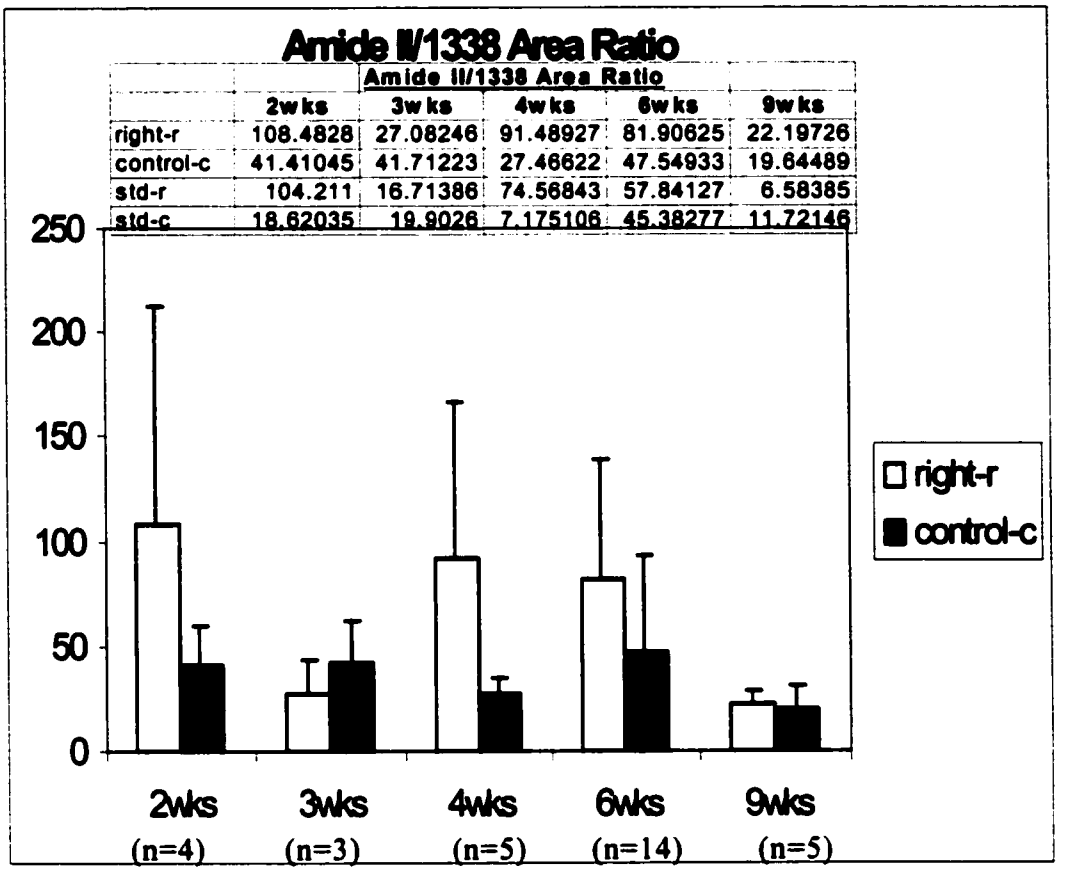

Fig. 9-2: Amide II/1338 cm^{-1} peak ratio in rabbit OA model.

Discussion

The IR changes observed in this rabbit OA model were in agreement with that seen in both the human study and in the collagenase treated bovine cartilage. This validates the notion that these IR changes are true indicators of cartilage degradation. We did not however, see a linear change in either parameter with time. This may likely be caused by variability in the cartilage of the different rabbits.

These data demonstrate that the IFOP if used in conjunction with arthroscopy is capable of sensing in vivo changes in articular cartilage that arise from degradation

CHAPTER X

SUMMARY

To date, Magnetic Resonance Imaging (MRI) techniques provide the most popular means for diagnosis and treatment for articular cartilage disorders. MRI has the unique capability to evaluate cartilage non-invasively with a spatial resolution of 100 μm. This limit in resolution however makes it difficult for MRI to reproducibly measure early cartilage changes (38). Numerous studies have also been performed in an attempt to identify the optimum technique for the detection of cartilage disorders. The most commonly accepted MRI technique for imaging articular cartilage is a fat suppressed three-dimensional T1-weighted gradient echo technique (39). However, there are several limitations with this technique: the long imaging time, inadequate visualization of ligamentous and meniscal pathology, necessitating additional sequences (39-42). This makes noninvasive diagnosis of the early stages of degenerative joint diseases like osteoarthritis impossible by means of established MRI techniques.

The infrared absorbing nature of biomolecules, specifically proteins, have been well documented over the past 50 years. However, it was not until the late 1980s and 1990s that many new developments in instrumentation and computational methods have occurred. These new developments have drastically altered the field of biomedical IR spectroscopy. Nowhere was this more evident than at the recent 2002 Phototonics West (Biomedical Optics) meeting in San Jose, California. Currently, numerous minimally invasive and non-invasive biological applications involving FT-IR spectroscopy are being developed worldwide. Whether it involves using optical probes or new evanescent wave methods, IR spectroscopy has emerged as a valuable tool for medical diagnostics.

FT-IR systems are readily available and they offer cost effectiveness and portability (available for in-office medical diagnostics – unavailable for MRI) while attaining a high degree of precision and accuracy. Here we have applied FT-IR techniques to the analysis of extracellular matrix changes that accompany the development and progression of joint disease (OA).

The use and development of the IFOP for spectral analysis of articular cartilage in the 4000-900 cm-1 wavenumber (mid-IR) region has led to the determination of specific IR parameters that change with cartilage integrity (disease). These findings, as evidenced in human articular cartilage, a rabbit model of OA and in collagenase treated bovine cartilage were also verified using our FT-IR imaging gold standard. Although the IFOP uses reflectance methods that provide less spectral intensity when compared to transmissive methods (gold standard), the IFOP data sets still achieved good statistical results.

Despite the well-documented structure of cartilage, and as encouraging as these results are, there are specific precautions that need to be taken when using the IFOP. For articular cartilage, whether it is between the same species, the same gender, or the same age group, there is a substantial degree of variability. Variability in cartilage thickness, surface morphology, chondrocyte count, chondrocyte response and extracellur composition. Primarily genetic factors and subject lifestyle induce this variability. In light of this, and in the absence of appropriate multivariate data analysis techniques, I would limit IFOP in situ determination to comparisons within the same joint. Comparisons made between two separate joints based solely on two IR parameters may potentially lead to diagnostic error due to cartilage variability. Such errors could be avoided however, by

the use of multivariate techniques that catalog subtle spectral changes related to cartilage quality and that rely on very large data sets (library set) in order to make determinations on cartilage integrity. Precaution also needs to be taken during the sampling procedure. Probe tip displacements up to 100 microns are recommended. This should not adversely affect the articular surface. Under normal in vivo loading conditions, cartilage is usually exposed to strains of up to 10% (43).

Our findings using polarized light have also been very positive. Due to the 90° difference in the in-plane vibrations of amide I and amide II bands, we were able to quantitate the amide I/II area ratio as a valid measure of cartilage orientation. Using polarized light does provide us with another valuable technique capable of determining collagen disruptions that accompany disease progression. Additional equipment however would be needed in order to add a polarizer to our current IFOP set-up.

The value of FT-IR spectroscopy in medical diagnostics is clear. Although new and minimally invasive, the IFOP appears to provide a more direct and reliable approach in the detection of cartilage integrity. It offers good spatial resolution and the potential to detect early structural changes in surface collagens. It is especially suited for localized assessment of the quality of tissue-engineered cartilage and for the *in situ* distinction between good and bad cartilage during surgery. Further work however needs to be done in the development of a more foolproof determination method. Once this obstacle is surpassed, and if the IFOP can be used in conjunction with a polarizer then the IFOP shows great potential as a possible diagnostic tool for in situ determination of articular cartilage integrity.

BIBLIOGRAPHY

1. MRI Clinics of North America. Charles G. Peterfy, Vol 8 no. 2. May 2000.

2. Orthopaedic Basic Science. Edited by Sheldon R. Simon, MD. American Academy of Orthopaedic Surgeons, 1994, (Chapter 1: Mankin et al)

3. Articular Cartilage and Osteoarthritis. Raven Press, New York 1991.

4. Buckwalter, J.A. and Martin, J.A., Mankin, H.J. Synovial Joint Degeneration and the Syndrome of Osteoarthritis. AAOS Instructural Course Lectures, Vol. 49 2000.

5. American Academy of Orthopaedic Surgeons. 1992. Musculoskeletal Conditions in the United States. AAOS, Park Ridge, IL. pp 34-45 .

6. Buckwalter, J.A., Mankin, H.J. Articular cartilage II. Degeneration and osteoarthrosis, repair, regeneration, and transplantation. *J Bone Joint Surg* 1997;79A:612-632.

7. Buckwalter, J.A. and Martin, J.A. Degenerative joint disease. *Clin Symp* 1995;47:1-32.

8. Lippielo L, Hall D, Mankin HJ: Collagen synthesis in normal and osteoarthritic human cartilage. *J Clin Invest* 1977;59:593-600.

9. Mankin HJ, Thrasher AZ: Water content and binding in normal and osteoarthritic human cartilage. *J Bone Joint Surg* 1975:57A:76-80.

10. Mankin HJ, Lippielo L: Biochemical and metabolic abnormalities in articular cartilage from osteoarthritic human hips. *J Bone Joint Surg* 1970 :52A:424-434.

11. Billinghurst, R.C. Dahlberg L. , Ionescu M. Enhanced Cleavage of type II Collagen by Collagenases in Osteoarthritic Articular Cartilage. J. Clin. Invest vol 99, no. 7, April 1997, 1534-1545.

12. Buckwalter, J.A. and Mow V.C.. 1994. Injuries to cartilage and meniscus: sports injuries to articular cartilage. In Orthopaedic sports

medicine principles and practice. J.C. DeLee and D.J. Drez, editors. W.B. Saunders Company, Philadelphia. 82-107.

13.Collins DH. The Pathology of Articular and Spinal Diseases. London: Edward Arnold and Co 1949;76-9

14.Tyler JA. Cartilage Degradation. In:Hall BK, Newman SA eds. Cartilage molecular aspects. Boca Raton, FL: CRC Press, 1991; 213-256.

15.Barrett AJ. Proteinase inhibitors. Amsterdam: Elsevier, 1986.

16.Matrisian LM. Metalloproteinases and their inhibitors in matrix remodelling. TIG 1990; 6: 121-125.

17.Murphy G., Docherty AJP, Hembry RM, Reynolds JJ. Metalloproteinases and tissue damage. Br J Rheumatol 1991; 30 (Suppl):25-31.

18.Casal, H.L and Mantsch, H.H. (1984) Biochim. Biophys. Acta 779, 381-401.

19.Hester, R.E. and Girling, R.B. (1991) Spectroscopy of Biological Molecules, Royal Society of Chemistry, Cambridge.

20.Jackson, M and Mantsch, H.H. (1993). Spectrochim. Acta Rev. 15, 53-69.

21.Mendelsohn, R., Hassankhani, A., Dicarlo, E and Boskey, A. (1989 Calcif. Tissue Int. 44, 20-24.

22.Jackson, M. Choo, L. Watson, P. Halliday, W. Mantsch, H. Beware of connective tissue proteins: assignment and implications of collagen absorptions in infrared spectra of human tissues. *Biochimica et Biophysica Acta* 1270 (1995) 1-6.

23.Hollander, A. P., T. F. Heathfield, C. Webber, Y. Iwata, R. Bourne, C. Rorabeck, and A. R. Poole. 1994. Increased damage to type II collagen in osteoarthritic articular cartilage detected by a new immunoassay. *Journal. of. Clinical. Investigation.* 93:1722-1732.

24. Hidaka, C., Quitoriano M., Warren, R.F., Crystal, R.G. Enhanced matrix synthesis and in vitro formation of cartilage-like tissue by genetically modified chondrocytes expressing BMP-7. J. Orthop. Res. 19 (2001) 751-758.

25. Helder, M.N., Ozkaynak, E., Sampath, K.T., Luyten, F.P. Expression pattern of osteogenic protein-1(bone morphogenetic protein-7) in human and mouse development. J. Histochem. Cytochem. 43 (1995) 1035-1044.

26. Hogan, B.L. Bone morphogenetic proteins: multifunctional regulators of vertebrate development, Genes Dev. 10 (1996) 1580-1594.

27. Ozkaynak, E., Rueger, D.C., Drier, E.A., OP-1 cDNA encodes an osteogenic protein in the TGF-β family, EMBO J. 9 (1990) 2085-2093.

28. Wozney, J.M., Rosen, V. Celeste, A. J. Novel regulators of bone formation: molecular clones and activities, Science 242 (4885) (1988) 1528-1534, Dec. 16.

29. Chubinskaya, C., Merrihew, C. Cs-Szabo, G. Human articular chondrocytes express osteogenic protein-1, J. Histochem. Cytochem. 48 (2) (2000) 239-250, Feb.

30. Chen, P., Vukicevic, S., Sampath, K.T., Luyten, F.P. Bovine articular chondrocytes do not undergo hypertrophy when cultured in the presence of serum and osteogenetic protein. Biochem. Biophys. Res. Commun. 197 (1993) 1253-1259.

31. Flechtenmacher, J. Huch, K., Thonar, E.J. Recombinant human osteogenetic protein-1 is a potent stimulator of the synthesis of cartilage proteoglycans and collagens by human articular chondrocytes, Arthritis Rheum. 39 (1996) 1896-1904.

32. Louwerse, R.T., Heyligers, I.C., Klein-Nulend, J. Use of recombinant human osteogenetic protein-1 for the repair of subchondral defects in articular cartilage in goats, J. Biomed. Mater. Res. 49 (2000) 506-516.

33. Muehleman C., Bareither D., Huch K. Prevalance of degenerative morphological changes in the joints of the lower extremity. Osteoarthritis and Cartilage (1997) 5, 23-37.

34.Camacho, N.P.,West, P.A., Torzilli, P.A., Mendelsohn, R. FTIR Microscopic Imaging of collagen and proteoglycan in bovine cartilage. Biopolymers, vol. 62, 1-8 (2001).

35.Billinghurst et al, 1997. Enhanced cleavage of type II collagen by collagenases in osteoarthritic articular cartilage. *J. Clin. Invest.* Vol. 99, 1534-1545.

36.Lazarev, Y., Lazareva, A.V. Infrared spectra and structure of synthetic polypeptides. Biopolymers, vol. 17, 1197-1214 (1978).

37.Ander Hulth et al, Acta Orthop. Scandinav. 41: 522-530 (1970).

38.Tyler, J.A., Watson, P.J., et al. Detection and monitoring of progressive degeneration of osteoarthritic cartilage by MRI. Acta Orthop Scand 1995; 66 Suppl 2: 130-9.

39.Article: Magnetic Resonance Imaging of Articular Cartilage Defects and Repair - Dr. Vladimir Bobic (International Society of Arthroscopy, Knee Surgery and Orthpaedic Sports Medicine.

40.Kneeland JB. MR imaging of articular cartilage and of cartilage degeneration. In: Stoller DW. Magnetic Resonance Imaging in Orthopaedic & Sports Medicine. CD-ROM. Lippincott-Raven Publishers, 1997.

41.Levy AS, Lohnes J, Sculley S, LeCroy M, Garrett W. Chondral delamination of the knee in soccer players. Am J Sports Med 1996; 24(5):634-9.

42.Linklater JM, Potter HG. Imaging of Chondral Defects. In: Miller M, Guest Ed. Treatment of Chondral Injuries. In: Fu F, ed. Operative Techniques in Orthopaedics. Philadelphia, PA: Saunders. 1997; 7(4):279-288.

43.Mauck, RL., Soltz, MA., et al. Functional Tissue Engineering of Articular Cartilage Through Dynamic Loading of Chondrocyte-Seeded Agarose Gels. Transactions of the ASME, vol. 122, JUNE 2000.